Supplementary Figure Legends and Supplementary Figures

Article Title:	Cell-specific histone modification maps link schizophrenia risk to the neuronal epigenome
Corresponding Author:	Schahram Akbarian Panos Roussos Gabriel Hoffman
Manuscript #:	NN-RS60953C

Supplementary Item & Number	**Title or Caption**
Supplementary Figure 1	**Quality control parameters**
Supplementary Figure 2	**Cell type and homogenate ChIP-seq data pipeline**
Supplementary Figure 3	**Contribution of peak regions from every sample to consolidated dataset peak regions.**
Supplementary Figure 4	**Similarity of cell type and homogenate data sets with Roadmap Epigenomics Project (REP) homogenates**.
Supplementary Figure 5	**Visualization of cell and tissue specificity in neuronal, non-neuronal and homogenate chromatin**
Supplementary Figure 6	**Cell composition analyses**.
Supplementary Figure 7	**Visualization ChIP-Seq data for representative neuronal and non-neuronal genes**
Supplementary Figure 8	**QTL enrichments**
Supplementary Figure 9	**Enrichment of heritability for brain and non-brain related phenotypes within non-overlapping regions of cell type and homogenate peaks.**
Supplementary Figure 10	**Coefficients of enrichments of heritability for schizophrenia within cell- and tissue-specific histone peaks**
Supplementary Figure 11	**Principal components analysis of cell type and homogenate datasets**
Supplementary Figure 12	**Cell specific hQTLs and hQTLs overlap with GWAS**
Supplementary Figure 13	**Functional enrichments for genes near significant hQTLs**
Supplementary Figure 14	**Differential modification analysis**
Supplementary Figure 15	**Differential modification analysis: Brain region specific**
Supplementary Figure 16	**Functional annotation of cell specific and brain region specific peaks.**
Supplementary Figure 17	**Data integration of neuronal and non-neuronal ChIP-Seq peaks (PFC and ACC) with transcription start sites and gene expression**
Supplementary Figure S18	**ChIP-PCR quality controls**
Supplementary Figure S19	**Gating for Fluorescence-activated cell sorter (FACS) collecting immunotagged NeuN+ and NeuN- nuclei**

SUPPLEMENTARY FIGURES LEGENDS

Figure S1: Quality control parameters. **(A)** Sequencing depth of n=17 and 19 individuals for celltype and homogenate data sets respectively. **(B)** Fragment lengths using SPP (see methods.) **(C)** Normalized strand coefficient obtained from SPP output file. All QC parameters have been group by data types: ACC neuronal, PFC neuronal, ACC neuron-depleted, PFC neuron-depleted and PFC HBCC homogenate for H3K4me3 and H3K27ac marks. **(D)** Irreproducible discovery rate (IDR) for PeakSeq(blue), SPP(green) and MACS2(orange) peak callers for peaks called on 3 random samples of consolidated PFC neuronal data set.

Figure S2: Cell type and homogenate ChIP-seq data pipeline. Mapping and QC: Flowchart demonstrating the QC of raw ChIP-Seq FASTQ files and consolidating the QCed files. Peak calling methods comparison: Steps to determine the best peak caller on consolidated datasets. Peak calling: Steps to call peaks on consolidated data sets**.** Quantification and covariates analysis: Quantifying the reads counts in determined peak regions and decomposing the contribution of the multiple sources of variations in the combined dataset. Differential modification and pathway analysis: Steps to determine the peak regions that have significant $\log_2$ fold-change in different cell types and brain regions.

Figure S3: Contribution of peak regions from every sample to consolidated dataset peak regions. (A,C) No. of peaks with $\log_2$cpm >1 that are present in at least 'n' individuals (n=17 for cell type and 11 for homogenate datasets).**(B,D)** Bar plot of no of peaks ($\log_2$cpm >1) of each sample that are contributing to consolidated datasets peaks.

Figure S4: Similarity of cell type and homogenate data sets with Roadmap Epigenomics Project (REP) homogenates. (top)

Box plots illustrates measured similarity (Jaccard index) of peak regions of 5 consolidated data sets (PFC neuronal; n=17(17), ACC neuronal; n=14(17), PFC neuron-depleted; n=17(17), ACC neuron-depleted n=15(15) and PFC tissue; n=11(17) from each mark H3K4me3(H3K27ac)) to 10(7) brain tissues in red and 107(84) non-brain tissues in grey from the Roadmap Epigenomics Project[5] for H3K4me3 (H3K27ac.) Box plots' black horizontal line correspond to the median value of jaccard

index values of our datasets with REP brain tissues and REP non-brain tissues respectively. The vertical line above and below box shows the 1.5IQR of upper quartile and 1.5IQR of lower quartile of jaccard index with REP tissues for a given dataset. Tissues with jaccard index values exceeding the 1.5IQR are shown as black dots. (bottom) Jaccard indices for the 5 consolidated H3K27ac data sets (PFC neuronal; n=17, ACC neuronal; n=17, PFC neuron-depleted; n=17, ACC neuron-depleted n=15 and PFC tissue; n=17) to (left) Sun et al.[10] H3K27ac from cortical homogenates and (right) Ng et al.,[11] H3K9ac from cortical homogenates.

Figure S5: Visualization of cell and tissue specificity in neuronal, non-neuronal and homogenate chromatin. PCA of pairwise correlations between each pair of ChIP-Seq experiments based on $\log_2$ cpm matrix from each mark. **(A)** Visualization of first two principal components where each data point is colored by cell type: neuronal chromatin in blue n=31(34) independent samples of neuron-depleted chromatin, n=32(32) independent samples in golden depicting the cell type and tissue n=11(17) independent samples in black **(B)** brain region: PFC in pink, n=45(51) independent samples and ACC in green, n=29(32) independent samples with no clear clustering for H3K4me3(H3K27ac) in left(right) panels.

Figure S6: Cell composition analyses. Scatter plot of estimated NeuN- fraction and first principal component (PC1) of histone ChIP-seq from sorted $NeuN^+$ and $NeuN^-$ nuclei and homogenate samples. These fractions were obtained using R library "cellmix" which uses Non-negative matrix factorization on RPKM matrix (rows are identified ChIP-seq genomic regions and columns are samples) and our neuronal and neuron-depleted chromatin signatures as basis set. PCA was done on pairwise correlations between each pair of ChIP-Seq samples (H3K4me3, our $NeuN^+$ and $NeuN^-$ nuclei and homogenate datasets (N=74), REP(N=2); H3K27ac, our $NeuN^+$ and $NeuN^-$ nuclei and homogenate datasets (N=83), REP(N=2) and Sun et.al (N=53) samples) based on $\log_2$ cpm matrix from each mark. We show PC1 vs $NeuN^-$ fraction for all samples: $NeuN^+$ in blue, $NeuN^-$ in golden, HBCC cortical tissue homogenate in black, Roadmap Epigenomics Project (REP) cortical tissue homogenate[5] in red, Sun et.al. [10] cortical homogenate in orange.

Figure S7: Visualization ChIP-Seq data for representative neuronal and non-neuronal genes. (A-B) Visualization of genome coverage of PFC neuronal, n=17(17) and PFC non-neuronal, n=17(17) data

sets (one dataset per brain) for neuronal gene: CAMK2A (A) and (B) non-neuronal gene OLIG1 from H3K4me3(H3K27ac) mark shown in upper track and bottom track respectively ; results shown are representative for 17/17 brains.

Figure S8: QTL enrichments. Fold enrichment of H3K27ac (left) and H3K9ac QTL's (right) identified in PFC homogenates and peaks called on neuronal (blue) and non-neuronal (golden) cell type consolidated datasets and differentially modified peaks labeled as "DiffBind neurons" (blue) and "DiffBind non-neurons" (golden) for (A) H3K27ac and (B) H3K4me3, respectively. Each bar shows a single value (the enrichment score) and its standard error. H3K4me3, N (brains) = 17 PFC $NeuN^+$, 17 PFC $NeuN^-$, 11 PFC tissue homogenate, and H3K27ac N (brains) = 17 PFC $NeuN^+$, 17 PFC $NeuN^-$, 17 PFC tissue homogenate.

Figure S9: Enrichment of heritability for brain and non-brain related phenotypes within non-overlapping regions of cell type and homogenate peaks. Heatmap of $-\log_{10}$Pvalue of enrichment from LD-score regression to partitioned heritability to test the genetic variants contributing to 18 brain and non-brain-related phenotypes were enriched for non-overlapping regions of PFC and ACC neuronal (blue) in block 1,2 and PFC and ACC neuron-depleted (golden) with PFC tissue homogenate '1' dataset of present study, '2' REP Roadmap Epigenomics Project and '3' dataset from ref.[10] (only for H3K27ac); and vice-versa in block 3 and 4 for H3K4me3 (**A**) and H3K27ac (**B**).

Figure S10: **Coefficients of enrichments of heritability for schizophrenia within cell- and tissue-specific histone peaks.** Bar plot of coefficient of LD-score regression for PFC $NeuN^+$, ACC $NeuN^+$ in blue and PFC $NeuN^-$, ACC $NeuN^-$ in gold, and ACC and PFC bulk tissue (homogenate) including our HBCC samples and Roadmap Epigenomics Project (REP)[5] and Sun et.al. [10] data for (A) H3K4me3 and (B) H3K27ac. Each bar shows a single value (the single LD score coefficient) and its standard error. H3K4me3, N (brains) = 17 PFC $NeuN^+$, 14 ACC $NeuN^+$, 17 PFC $NeuN^-$, 15 ACC $NeuN^-$, and 11 PFC tissue homogenate; H3K27ac. N (brains) = 17 PFC $NeuN^+$, 17 ACC $NeuN^+$, 17 PFC $NeuN^-$, 15 ACC $NeuN^-$, 17 PFC tissue homogenate (HBCC).

Figure S11: Principal components analysis of cell type and homogenate datasets. PCA of pairwise correlations between each pair of ChIP-Seq experiments based on $\log_2$ cpm matrix of all genomic

regions and matrix with excluding the columns for peak regions from sex chromosomes (chrX and chrY). (**A**) from H3K4me3 mark (**B**) from H3K27ac mark. Right panel of (A,B) show PC1 and PC4 where each data point is colored by cell type: neuronal in blue, neuron-depleted in golden and homogenates in black. Left panel in (**A**) shows clustering of these points by sex, colored as females in orange and males in light blue where clustering by sex disappears after removal of sex chromosomal peak regions. H3K4me3 (H3K27ac) n=31(34) independent samples of neuron-depleted chromatin, n=32(32) independent samples in golden depicting the cell type and tissue n=11(17) independent samples in black

Figure S12: Cell specific hQTLs and hQTLs overlap with GWAS. A) Number of significant hQTLs discovered in H3K4me3- (top row) and H3K27ac-tagged sequences (bottom row) in PFC NeuN+, ACC $NeuN^+$, PFC $NeuN^-$, ACC $NeuN^-$ and PFC homogenate samples. Sample sizes (N) provided in parenthesis. **B)** hQTLs-GWAS overlap: Number of significant loci (from PGC SCZ GWAS) overlapping with cell and tissue specific hQTLs (qvalue < .05) for every dataset:- PFC $NeuN^+$, ACC $NeuN^+$, PFC $NeuN^-$, ACC $NeuN^-$ and PFC HBCC tissue homogenate for both histone marks. Number of loci were determined by evaluating the overlap of GWAS –SCZ lead SNP with SNPs in LD (R^2 > 0.8) with hQTLs (qvalue <0.05.)

Figure S13: Functional enrichments for genes near significant H3K27ac hQTLs. Bar plots of functional enrichments computed using GREAT of significant PFC neuronal, ACC neuronal, PFC neuronal, PFC neuron-depleted ('non-neurons'), ACC neuron-depleted ('non-neurons) and PFC homogenate hQTLs (RASQUAL q value < 0.05) depicting top 20 pathways for GO Biological process with $-\log_{10}$ p-value. N (brains) = 17 PFC $NeuN^+$, 17 ACC $NeuN^+$, 17 PFC $NeuN^-$, 15 ACC $NeuN^-$, 17 PFC tissue homogenate (HBCC).

Figure S14: Differential modification analysis. (A-B) Volcano plot showing the distribution of $-\log_{10}$p-value and $\log_2$fold-change obtained from differential modification analysis A) Cell Specific: peaks in blue and golden are enriched in neuronal and neuron-depleted chromatin, respectively. Non-significant regions are shown in black for H3K4me3 and H3K27ac marks. Bottom panel shows the distribution of $\log_2$fold-change of these enriched regions for both marks. B) Brain region

specific: peaks in green and pink show enrichment for ACC and PFC respectively in neuronal cell type data for H3K4me3 (H3K27ac) marks. Bottom panel show the distribution of log_2fold-change of these enriched regions for both marks. H3K4me3 N (brains) = 17 PFC $NeuN^+$, 14 ACC $NeuN^+$, 17 PFC $NeuN^-$, 15 ACC $NeuN^-$, and 11 PFC tissue homogenate; H3K27ac N (brains) = 17 PFC $NeuN^+$, 17 ACC $NeuN^+$, 17 PFC $NeuN^-$, 15 ACC $NeuN^-$, 17 PFC tissue homogenate (HBCC).

Figure S15: Differential modification analysis: Brain region specific (A) Counts of brain region specific peaks in neuronal cells for H3K4me3 and H3K27ac. Differentially histone modification analysis was performed on the normalized read counts matrix with columns as genomic regions 128,467 (147,539) and 4 types of samples PFC neuronal, ACC neuronal, PFC neuron-depleted and PFC neuron-depleted from 17 individuals as rows 63 (66) after QC for H3K4me3 (H3K27ac.) In the brain region analysis, the largest effect is found in the H3K27ac - neuronal comparison. **(B)** Examining the Cell Type specificity of identified Brain Region specific peaks. Distribution of log_2 fold change of region specific peaks in blue and gold are neuronal and non-neuronal cell types respectively. This plot depicts the presence of non-neuronal peak regions in PFC neuronal, ACC neuronal region specific peaks. **(C)** Correlation plot of log_2FC of region specific peaks with log_2FC from cell specific differential modification analysis. **(D)** Counts of brain region specific peaks in neuron-depleted chromatin for H3K4me3 and H3K27ac.

Figure S16: Functional annotation of cell specific and brain region specific peaks. Genomic feature distribution of ACC neuronal, PFC neuronal, ACC neuron-depleted, PFC neuron-depleted and PFC HBCC homogenate. Distribution was evaluated across seven distinct categories: promoter, intron, exons, 3' UTR, 5'UTR, and two types of intergenic sequences: ≤3Kb and >3kb ('distal') from nearest gene body plus minimum of 5Kb distance from nearest TSS.

Figure S17: Data integration of neuronal and non-neuronal ChIP-Seq peaks (PFC and ACC) with transcription start sites and gene expression. Chip-Seq counts enrichment of (**A**) H3K4me3 and (**B**) H3K27ac within 15 Kb downstream and upstream of transcription start site (TSS) for genes in each of 5 sets sorted by expression level in post mortem brain homogenate from the CommonMind Consortium (see Methods).

Figure S18: ChIP-PCR quality controls. Bar graph (top) (N = 5, mean ± SD) and (middle) qPCR signal traces, representative for 5/5 samples, showing the enrichment of H3K4me3 (left) and H3K27ac (right) in neuronal $NeuN^+$ nuclei fraction as compared to non-neuronal NeuN- nuclei for the neuronal gene *GRIN2B*, but not for negative control *HBB* beta-globin gene. Primer Sequence for *Grin2B*: forward: 5' - TCC TCT TCC ATT CAG GTT GG - 3'; reverse: 5' - GGC TAT ACC ATT CCT GGG ACA - 3'. Primer Sequence for *HBB*: forward: 5' - TCC CCA GGT AGT TCC CTT TT - 3'; reverse: 5' - TTC AAG GCC CTG TAG TTG CT - 3'. (Bottom) H3K4me3 and H3K27ac ChIPseq map tracks show signal from *GRIN2B* (neuronal mark), *GFAP* (astrocyte mark), and *HBB* (negative control) genes from both $NeuN^+$ and $NeuN^-$ nuclei. Notice the cell-type specificity for both histone marks.

Figure S19: FACS gating. Representative FACS gating panels for human cortical nuclei immunotagged with NeuN antibody. Gating parameters to maximize specificity of NeuN+ sorting with complete separation from NeuN- population.

Figure S1

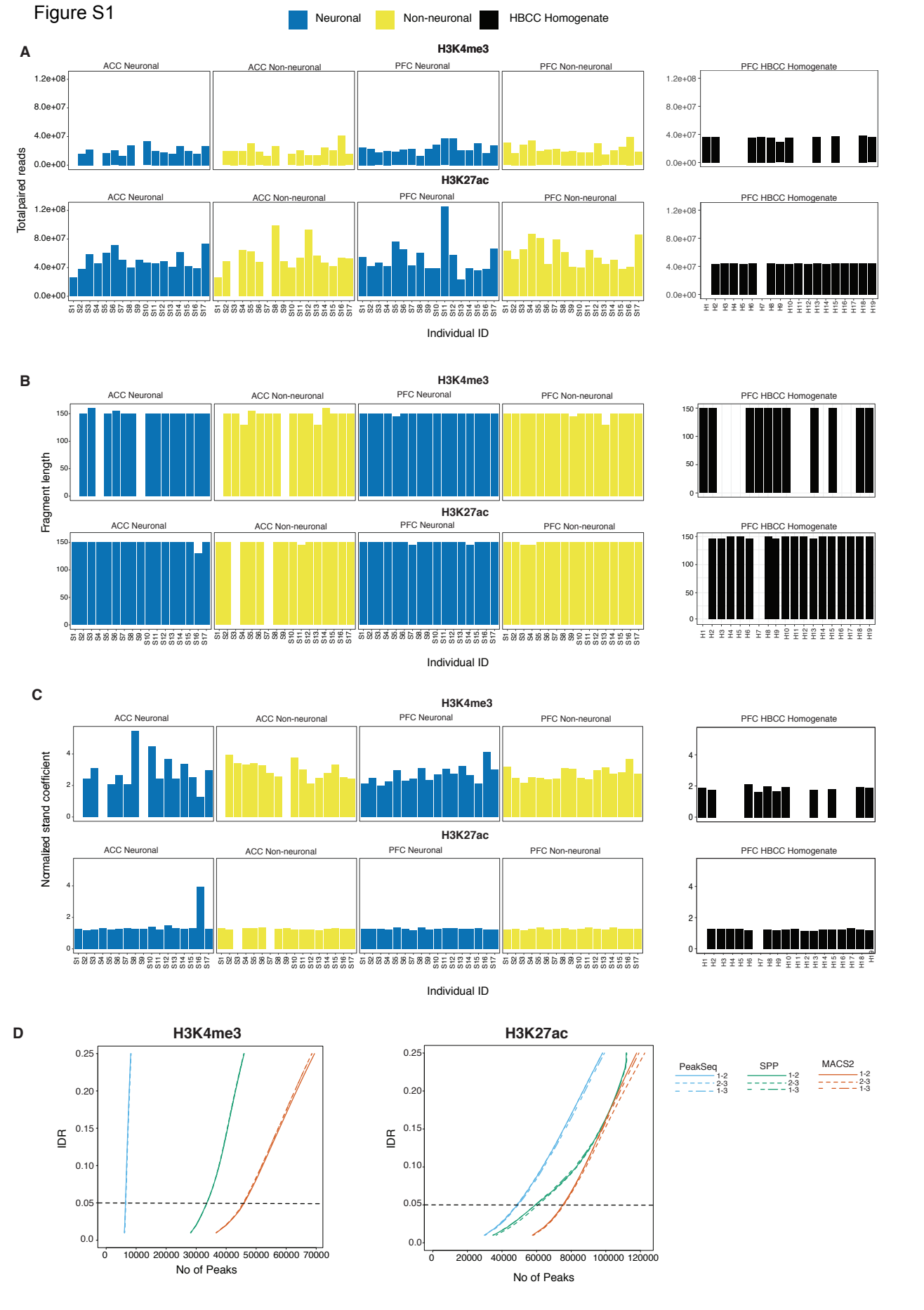
Neuronal
Non-neuronal
HBCC Homogenate
A
H3K4me3
H3K27ac
ACC Neuronal
ACC Non-neuronal
PFC Neuronal
PFC Non-neuronal
PFC HBCC Homogenate
Totalpaired reads
Individual ID
B
Fragment length
C
Normalized stand coefficient
D
H3K4me3
H3K27ac
IDR
No of Peaks
PeakSeq
SPP
MACS2
1-2
2-3
1-3

Figure S2

Cell type and homogenate ChIP-Seq pipeline

Mapping and QC

157 FASTQ files from sequencer
↓
Alignment to genome hg19 (***BWA***)
↓
Filtering out duplicates, subsampling (***Picard,samtools***) subsampling BAMs to median number of paired end reads for H3K4me3=13M and H3K27ac=21M
↓
Variant calling on BAMs (***bcftools,GATK***) concordance analysis to identify mislabeled samples

QC of BAMs (***SPP***)

Mapped reads, fragment length, NSC and RSC parameters to filter out the BAMS with low quality

Irreproducible Discovery Analysis Rate (***IDR***)

Consolidate PFC neuronal samples as
1. H3K4me3-PFC neuronal
2. H3K27ac-PFC neuronal

Subsample 3 BAMs from1,2 consolidated bams

Call peaks (MACS2, PeakSeq and SPP) on subsampled BAMs to assess the reproducibility of peakcallers

Run IDR on peak files from each peakcaller

Consolidating datasets

Subsetting of QCed BAMs from 157 samples and 20 input-controls (***bamtools***)

	63 cell type and 11 homogenate H3K4me3 samples	66 cell type and 17 homogenate H3K27ac samples	18 cell type and 2 homogenate input-control samples
Cell type	1. H3K4me3-PFC neuronal 2. H3K4me3-ACC neuronal 3. H3K4me3-PFC non-neuronal 4. H3K4me3-ACC non-neuronal	6. H3K27ac-PFC neuronal 7. H3K27ac-ACC neuronal 8. H3K27ac-PFC non-neuronal 9. H3K27ac-ACC non-neuronal	Cell.specific.input.bam
Homogenate	5. H3K4me3-PFC HBCC Homogenate	10.H3K27ac-PFC HBCC Homogenate	HBCC.homogenate.input.bam

Peak Calling

Call Peaks on consolidated BAMs (***MACS2***)

Narrow peaks
pvalue=0.1
samples=1-5 **H3K4me3** consolidated samples
control=Cell.specific.input.bam (HBCC.homogenate.input.bam)

Broad peaks
pvalue=0.1
samples=6-10 **H3K27ac** consolidated samples
control=Cell.specific.input.bam (HBCC.homogenate.input.bam)

Quantification of Chip-Seq signal

Generating Consensus signal bedtools (***R library GenomicRanges***)

H3K4me3 consensus signal
Union of 4 cell type and 1 homogenate narrowPeak files

H3K27ac-consensus signal
Union of 4 cell type and 1 homogenate broadPeak files

Quantification of H3K4me3, H3K27ac modified Chip-seq reads (***featurecounts***)

H3K4me3 $\log_2$ *counts per million matrix (cpm)*
samples = 63 cell type and 11 homogenate
saf = H3K4me3 consensus signal

H3K27ac $\log_2$ *counts per million matrix (cpm)*
samples = 66 cell type and 17 homogenates
saf = H3K27ac consensus signal

Outliers removal and covariate analysis

To identify outliers in the dataset

PCA of $\log_2$ cpm matrix of H3K4me3, H3K27ac

Quantifying % variance from each covariate for each mark (***VariancePartition***)

Input: H3K4me3 $\log_2$cpm matrix, H3K27ac $\log_2$cpm matrix

Visualization and statistical analysis of cell- and tissue specificity of peak regions

PCA of $\log_2$ cpm matrix to visualize cell type and tissue type specificity for H3K4me3, H3K27ac marks

Differential histone modification peak regions (***R library edgeR***)
Input: H3K4me3 $\log_2$cpm matrix , H3K27ac $\log_2$cpm matrix of cell type samples

Cell specificity	Tissue type specificity
Neuronal vs. Non-neuronal	ACC vs. PFC in neuronal samples ACC vs PFC in non-neuronal samples

Characterstics of identified peak regions

Annotation of peak regions ***(R library ChipSeeker)***

Input: narrowPeak, broadPeak files of consolidated cell type, HBCC homogenate datasets and cell and tissue specific peak regions from differential modification analysis.

Pathways analysis of peak regions (***GREAT***)

Input: narrowPeak, broadPeak files of consolidated cell type, HBCC homogenate datasets and cell and tissue specific peak regions from differential modification analysis.

Comparison of cell specific and HBCC homogenate peak regions

Pathways enrichment analysis of non-overlapping peak regions(***GREAT***)

Input: non-overlapping/unique regions of PFC neuronal, PFC non-neuronal and PFC HBCC homogenate narrowPeak(broadPeaks) files of H3K4me3(H3K27ac) mark.

sc-RNA seq identified cell type genes enrichment analysis(***ngsplot***)
Input:8 cell type and 2 HBCC homogenate consolidated BAMs genesets: neuronal and non-neuronal cell types (Regev et.al.)
Enrichment of BAMs for these genesets at a distance of 15Kb upstream and downstream fromTSS

Comparison of cell specific and HBCC homogenate dataset with existing brain epigenomic datasets

PFC,ACC homogenate REP peak regions and PFC homgenate from Sun et.al. and Ng et.al. peak regions

Jaccard Index b/w feature A & feature B (***bedtools***)
feature A: narrowPeak, broadPeak files of consolidated cell type, HBCC homogenate datasets
feature B: bed files of REP, Sun et.al., and Ng et.al. homogenate data

QTL peak regions enrichment in cell specific and HBCC homogenate peak regions

PCA and clustering of $\log_2$ cpm matrix of cell type, homogenate, data from HBCC and REP sun et.al.

Enrichment of neuropsychiatric diseases in cell specific and HBCC homogenate datasets

GWAS ***(LD-score regression)***
Input: narrowPeak, broadPeak files of consolidated cell type, HBCC homogenate datasets and cell and tissue specific peak regions from differential modification analysis.

Differential micrroarray and RNA seq gene expression (***ngsplot***)

Input:8 cell type and 2 HBCC homogenate consolidated BAMs genesets: genes of Autism, SCZ etc. from (Fromer et.al., Gandal et.al.)
Enrichment of BAMs for these genesets at a distance of 15Kb upstream and downstream from TSS

Figure S3

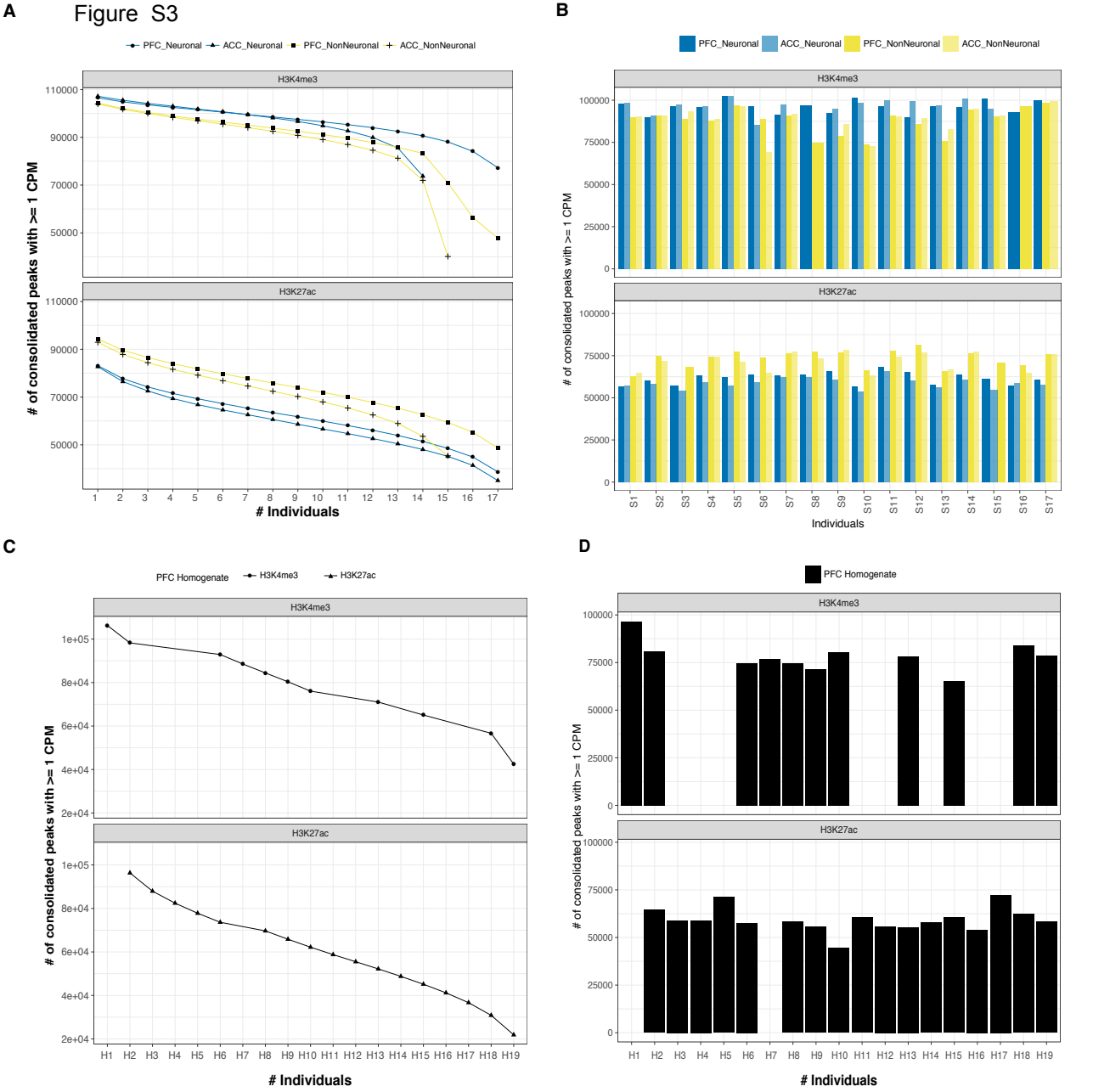
A
PFC_Neuronal
ACC_Neuronal
PFC_NonNeuronal
ACC_NonNeuronal
H3K4me3
H3K27ac
# of consolidated peaks with >= 1 CPM
Individuals
B
PFC_Neuronal
ACC_Neuronal
PFC_NonNeuronal
ACC_NonNeuronal
H3K4me3
H3K27ac
# of consolidated peaks with >= 1 CPM
Individuals
C
PFC Homogenate
H3K4me3
H3K27ac
# of consolidated peaks with >= 1 CPM
Individuals
D
PFC Homogenate
H3K4me3
H3K27ac
# of consolidated peaks with >= 1 CPM
Individuals

Figure S4

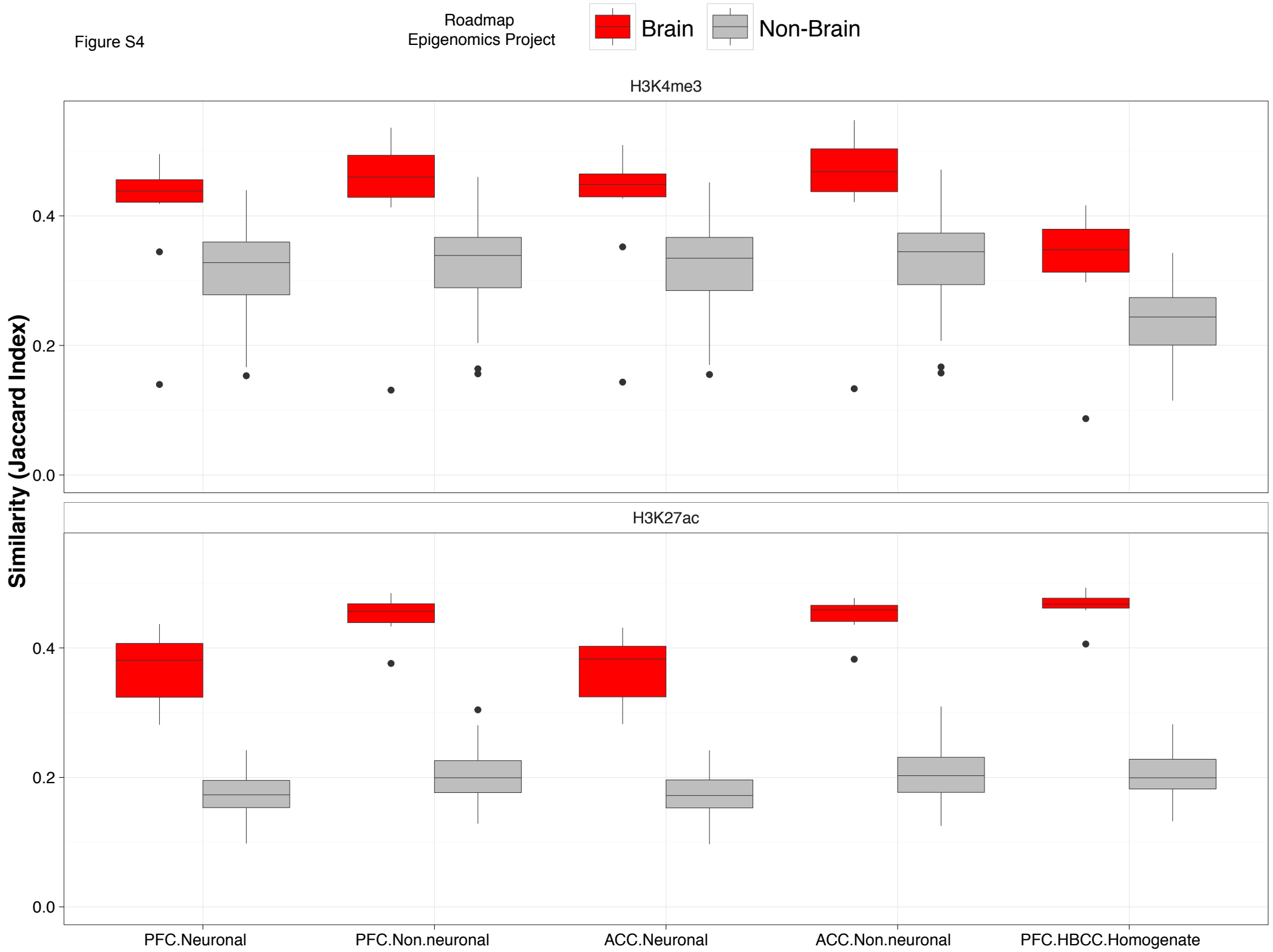
Roadmap
Epigenomics Project
Brain
Non-Brain
H3K4me3
H3K27ac
Similarity (Jaccard Index)
0.0
0.2
0.4
PFC.Neuronal
PFC.Non.neuronal
ACC.Neuronal
ACC.Non.neuronal
PFC.HBCC.Homogenate

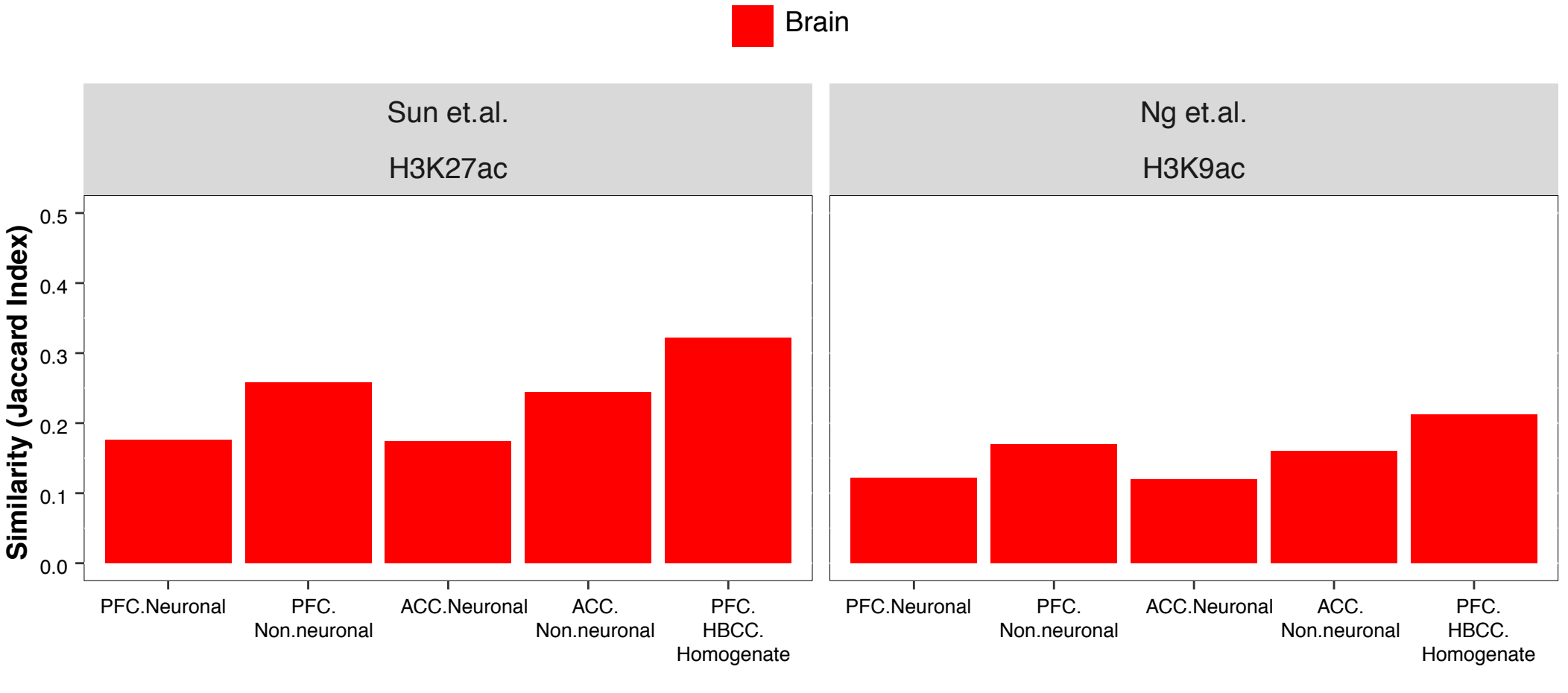
Brain
Sun et.al.
H3K27ac
Ng et.al.
H3K9ac
Similarity (Jaccard Index)
0.0
0.1
0.2
0.3
0.4
0.5
PFC.Neuronal
PFC.
Non.neuronal
ACC.Neuronal
ACC.
Non.neuronal
PFC.
HBCC.
Homogenate

Figure S5

A

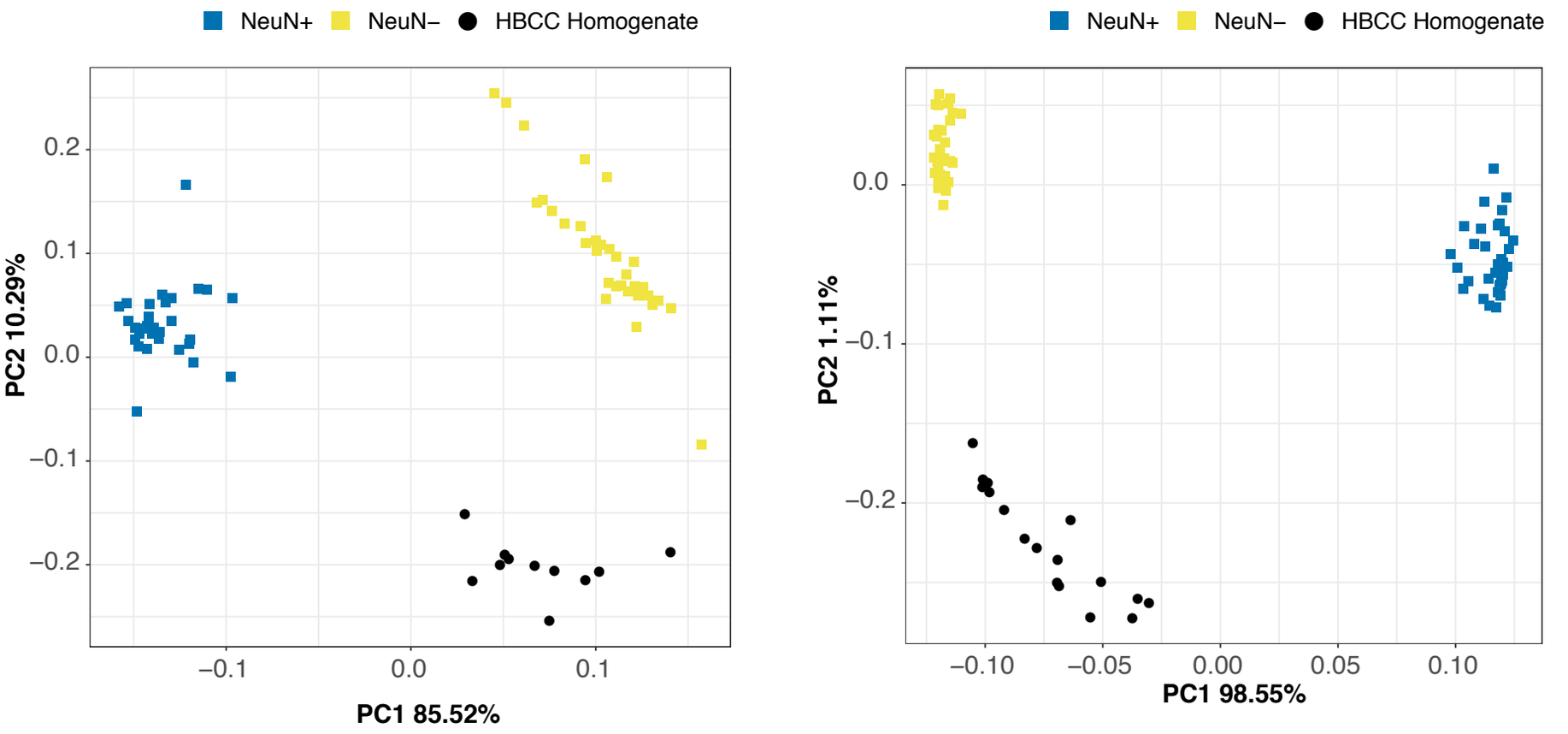
H3K4me3
H3K27ac
NeuN+
NeuN−
HBCC Homogenate
PC2 10.29%
PC1 85.52%
PC2 1.11%
PC1 98.55%

B

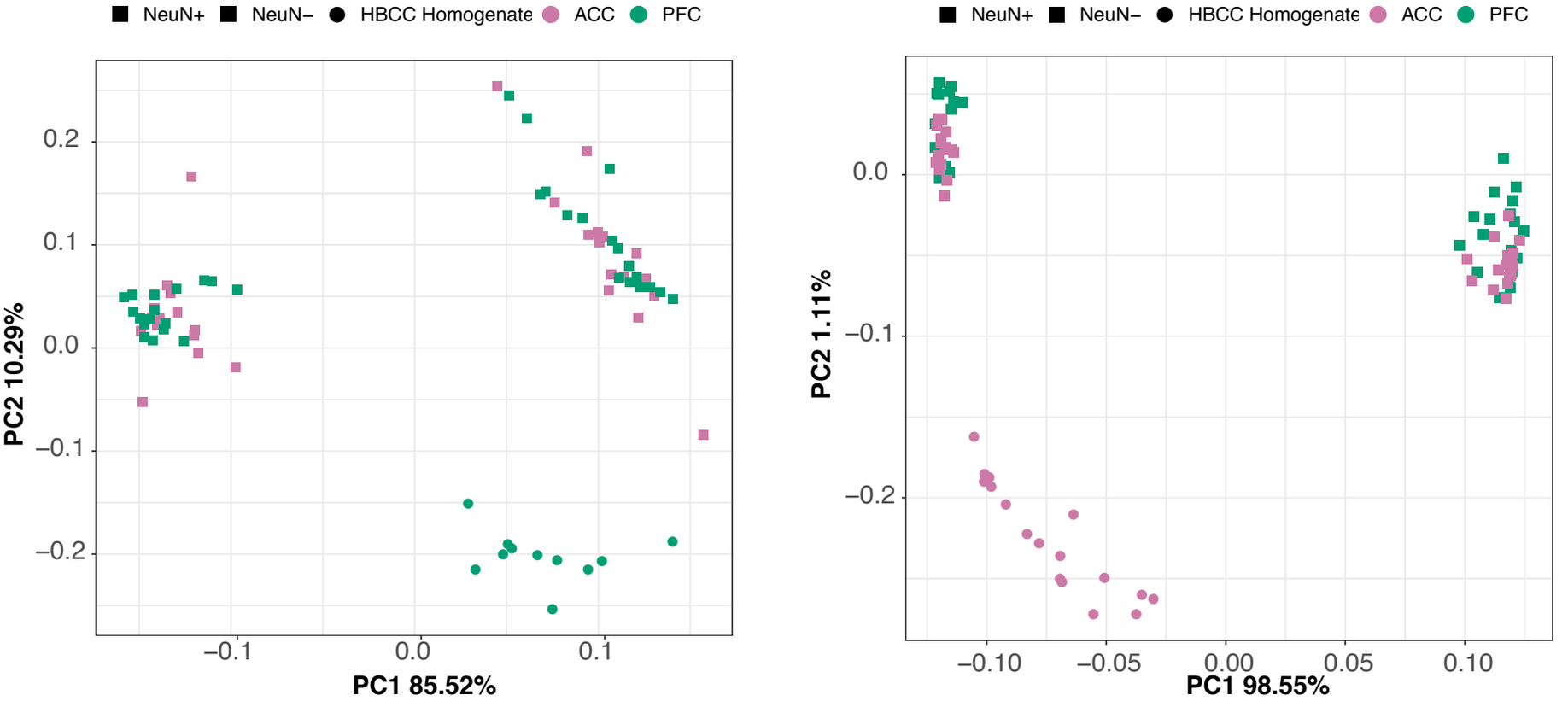
NeuN+
NeuN−
HBCC Homogenate
ACC
PFC
PC2 10.29%
PC1 85.52%
PC2 1.11%
PC1 98.55%

Figure S6

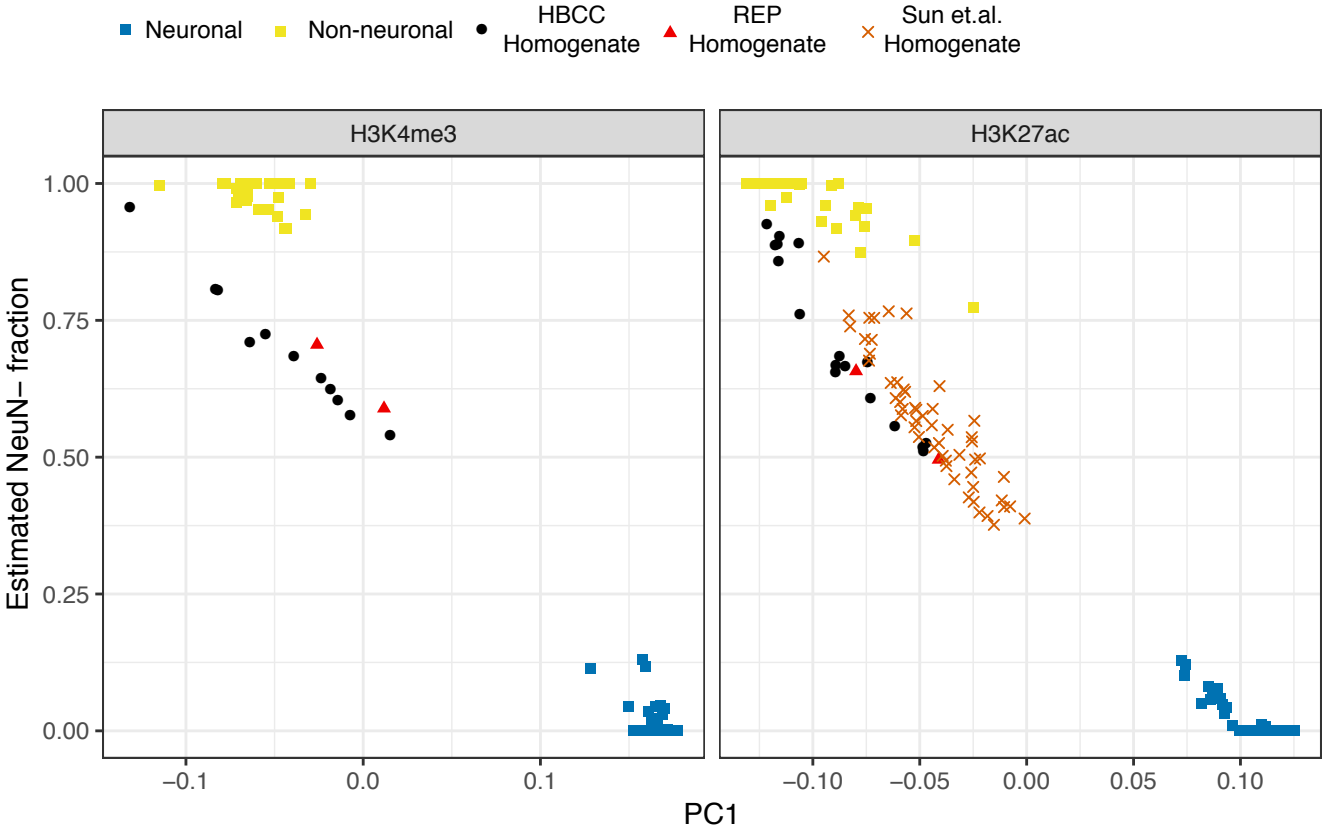
Neuronal
Non-neuronal
HBCC Homogenate
REP Homogenate
Sun et.al. Homogenate
H3K4me3
H3K27ac
Estimated NeuN− fraction
1.00
0.75
0.50
0.25
0.00
−0.1
0.0
0.1
−0.10
−0.05
0.00
0.05
0.10
PC1

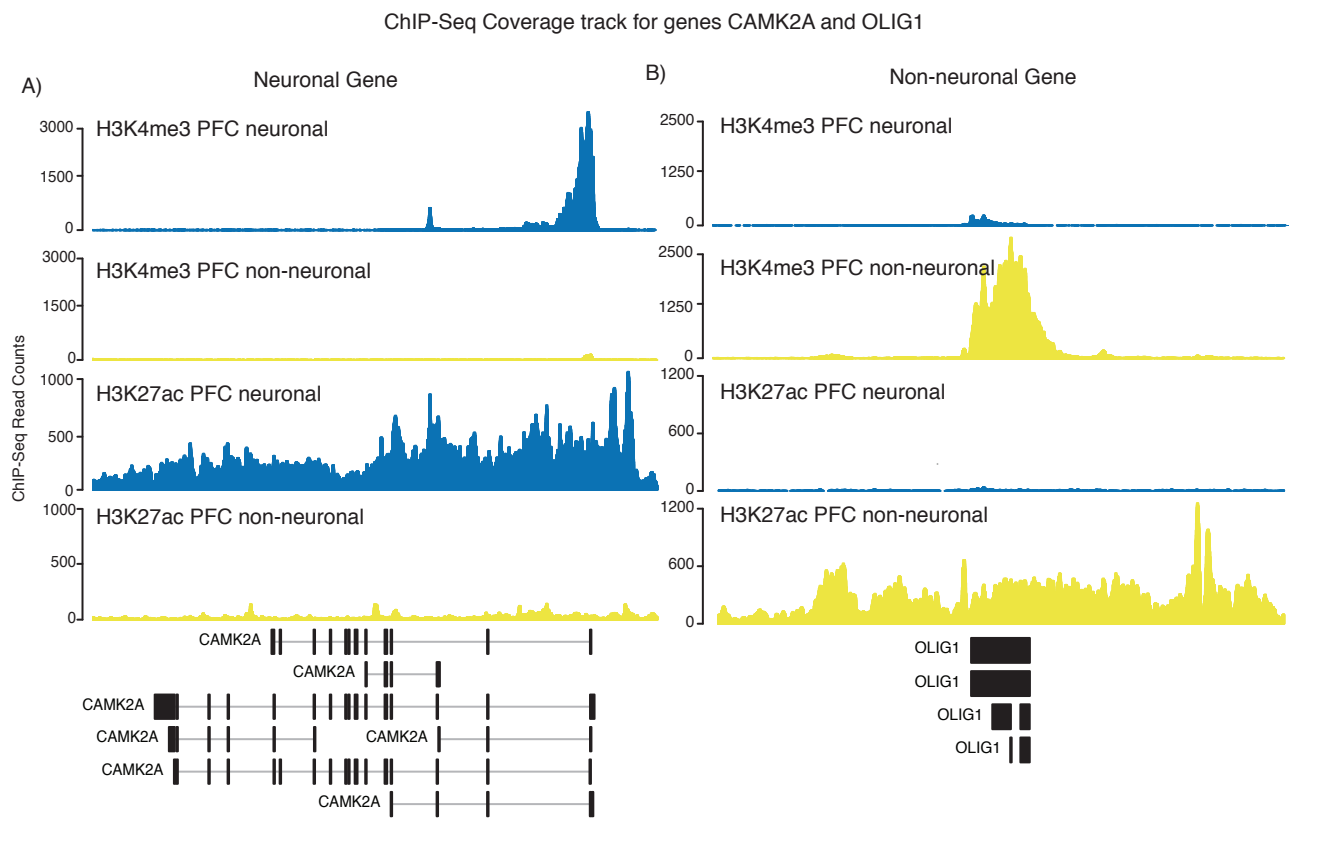
ChIP-Seq Coverage track for genes CAMK2A and OLIG1
A)
Neuronal Gene
B)
Non-neuronal Gene
ChIP-Seq Read Counts
H3K4me3 PFC neuronal
H3K4me3 PFC non-neuronal
H3K27ac PFC neuronal
H3K27ac PFC non-neuronal
3000
1500
0
2500
1250
1000
500
1200
600
CAMK2A
OLIG1

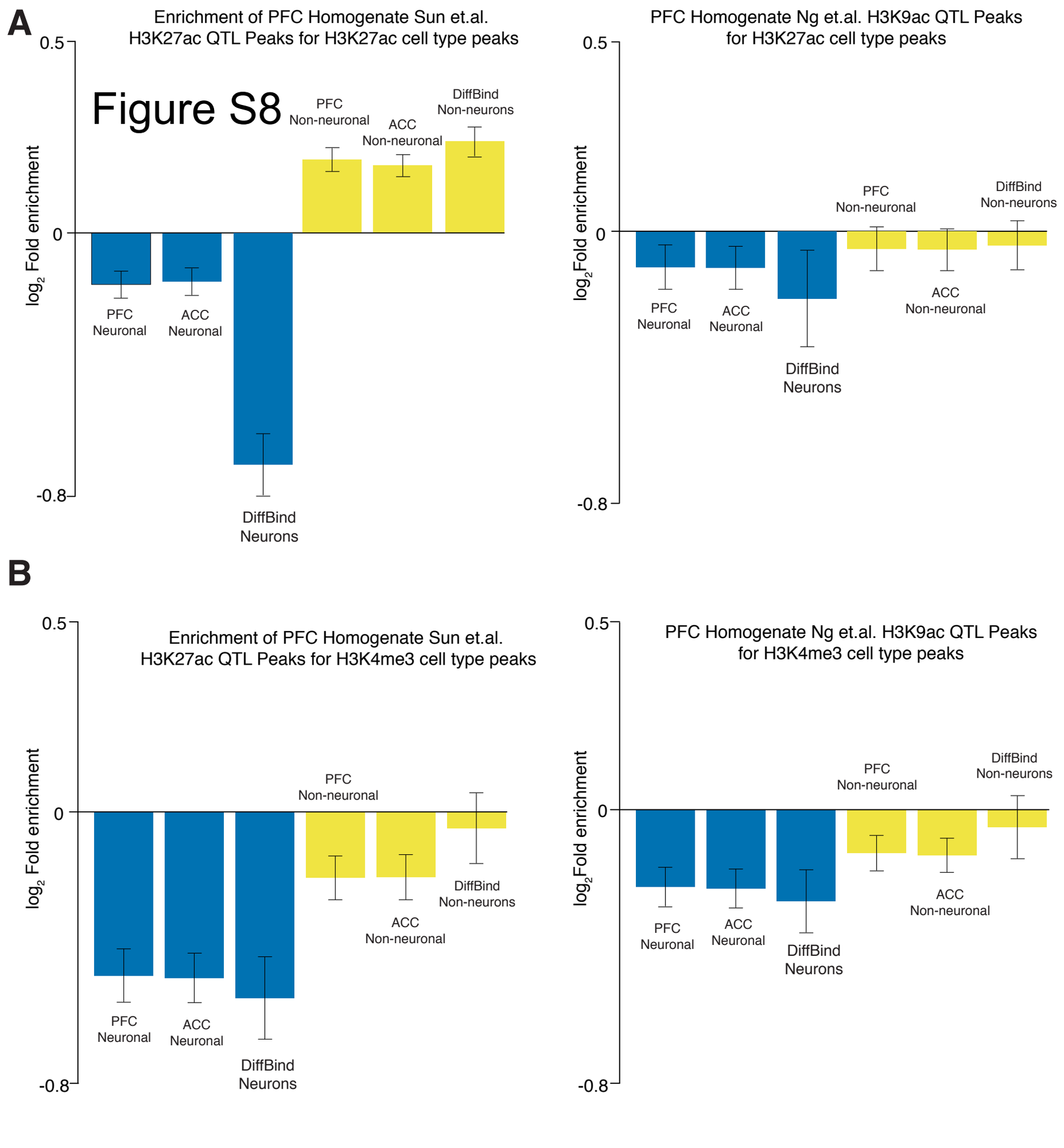
A
Enrichment of PFC Homogenate Sun et.al.
H3K27ac QTL Peaks for H3K27ac cell type peaks
Figure S8
0.5
0
-0.8
log2 Fold enrichment
PFC Neuronal
ACC Neuronal
DiffBind Neurons
PFC Non-neuronal
ACC Non-neuronal
DiffBind Non-neurons
PFC Homogenate Ng et.al. H3K9ac QTL Peaks
for H3K27ac cell type peaks
B
Enrichment of PFC Homogenate Sun et.al.
H3K27ac QTL Peaks for H3K4me3 cell type peaks
PFC Homogenate Ng et.al. H3K9ac QTL Peaks
for H3K4me3 cell type peaks

A Figure S9

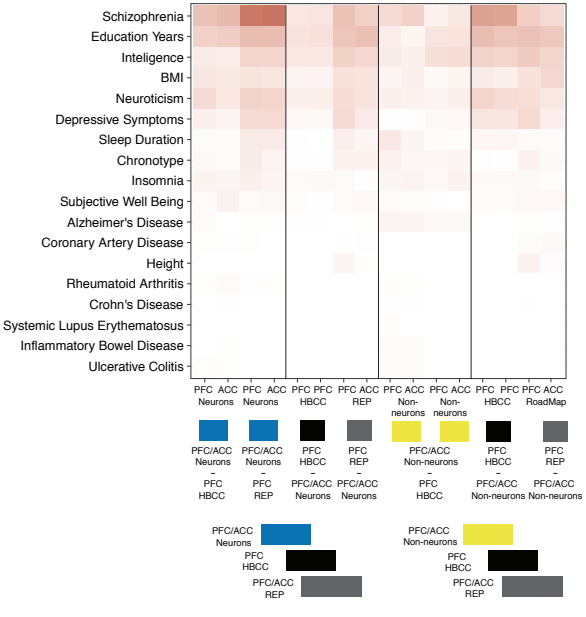
Figure S9
H3K4me3
Schizophrenia
Education Years
Inteligence
BMI
Neuroticism
Depressive Symptoms
Sleep Duration
Chronotype
Insomnia
Subjective Well Being
Alzheimer's Disease
Coronary Artery Disease
Height
Rheumatoid Arthritis
Crohn's Disease
Systemic Lupus Erythematosus
Inflammatory Bowel Disease
Ulcerative Colitis
PFC Neurons
ACC Neurons
PFC Neurons
ACC Neurons
PFC HBCC
PFC HBCC
ACC REP
PFC Non-neurons
ACC Non-neurons
PFC HBCC
PFC HBCC
ACC RoadMap
PFC/ACC Neurons – PFC HBCC
PFC/ACC Neurons – PFC REP
PFC HBCC – PFC/ACC Neurons
PFC REP – PFC/ACC Neurons
PFC/ACC Non-neurons – PFC HBCC
PFC HBCC – PFC/ACC Non-neurons
PFC REP – PFC/ACC Non-neurons
PFC/ACC Neurons
PFC HBCC
PFC/ACC REP
PFC/ACC Non-neurons
PFC HBCC
PFC/ACC REP

B

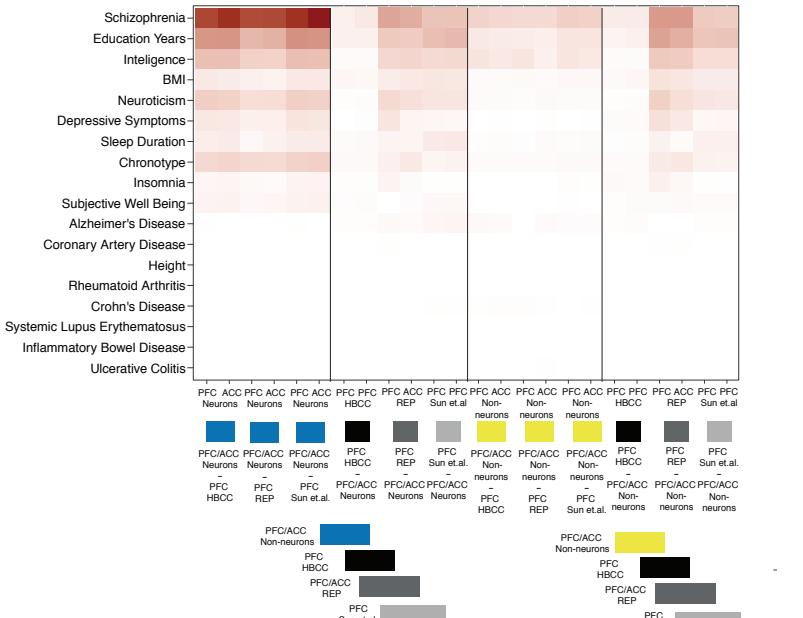
H3K27ac
Schizophrenia
Education Years
Inteligence
BMI
Neuroticism
Depressive Symptoms
Sleep Duration
Chronotype
Insomnia
Subjective Well Being
Alzheimer's Disease
Coronary Artery Disease
Height
Rheumatoid Arthritis
Crohn's Disease
Systemic Lupus Erythematosus
Inflammatory Bowel Disease
Ulcerative Colitis
PFC Neurons
ACC Neurons
PFC Neurons
ACC Neurons
PFC Neurons
ACC Neurons
PFC HBCC
PFC HBCC
PFC REP
ACC REP
PFC Sun et.al
PFC Sun et.al
PFC Non-neurons
ACC Non-neurons
PFC Non-neurons
ACC Non-neurons
PFC Non-neurons
ACC Non-neurons
PFC HBCC
PFC HBCC
PFC REP
ACC REP
PFC Sun et.al
PFC Sun et.al
PFC/ACC Neurons – PFC HBCC
PFC/ACC Neurons – PFC REP
PFC/ACC Neurons – PFC Sun et.al
PFC HBCC – PFC/ACC Neurons
PFC REP – PFC/ACC Neurons
PFC Sun et.al – PFC/ACC Neurons
PFC/ACC Non-neurons – PFC HBCC
PFC/ACC Non-neurons – PFC REP
PFC/ACC Non-neurons – PFC Sun et.al
PFC HBCC – PFC/ACC Non-neurons
PFC REP – PFC/ACC Non-neurons
PFC Sun et.al – PFC/ACC Non-neurons
PFC/ACC Non-neurons
PFC HBCC
PFC/ACC REP
PFC Sun et.al
PFC/ACC Non-neurons
PFC HBCC
PFC/ACC REP
PFC Sun et.al

Figure S10

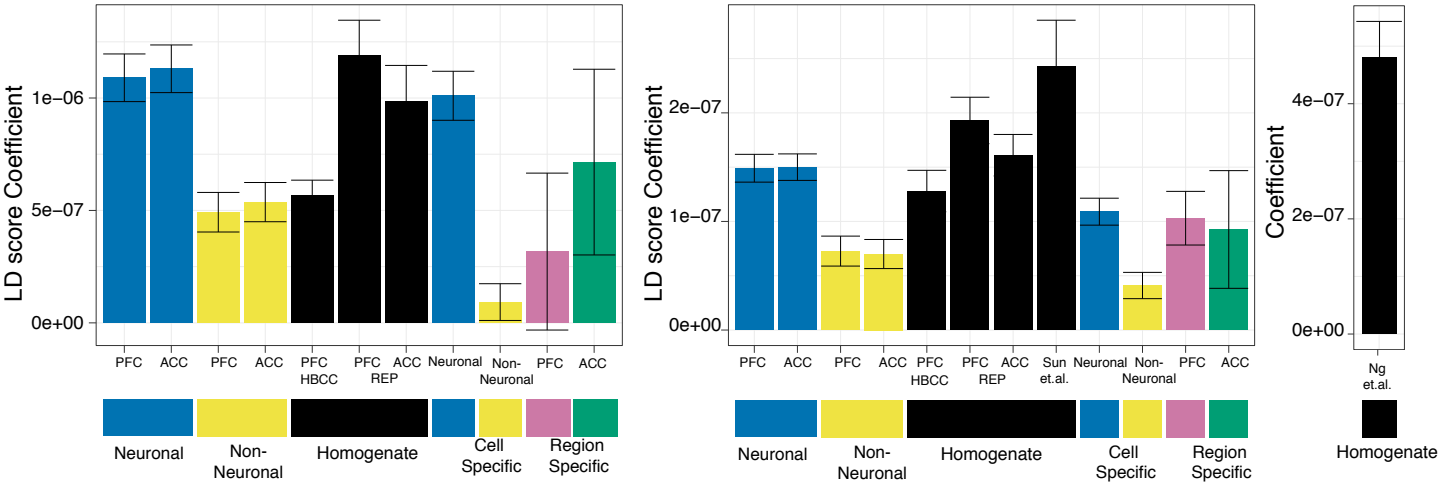
H3K4me3
H3K27ac
H3K9ac
LD score Coefficient
Coefficient
1e−06
5e−07
0e+00
2e−07
1e−07
4e−07
2e−07
0e+00
PFC
ACC
PFC
ACC
PFC HBCC
PFC REP
ACC
Neuronal
Non-Neuronal
PFC
ACC
Sun et.al.
Ng et.al.
Neuronal
Non-Neuronal
Cell Specific
Region Specific
Homogenate

A Figure S11

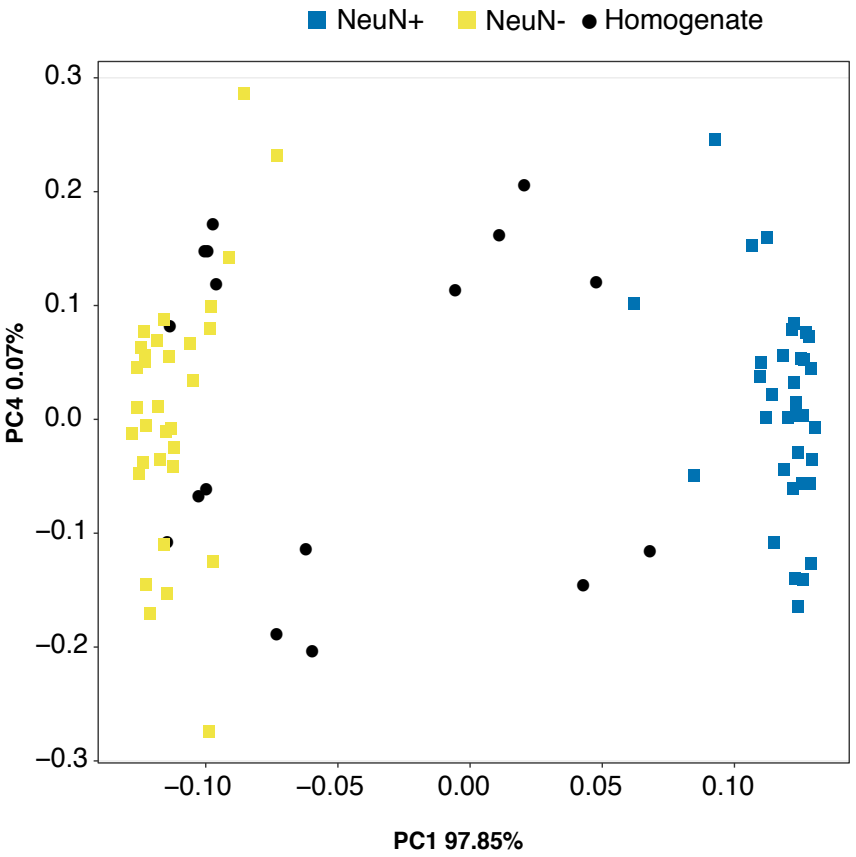

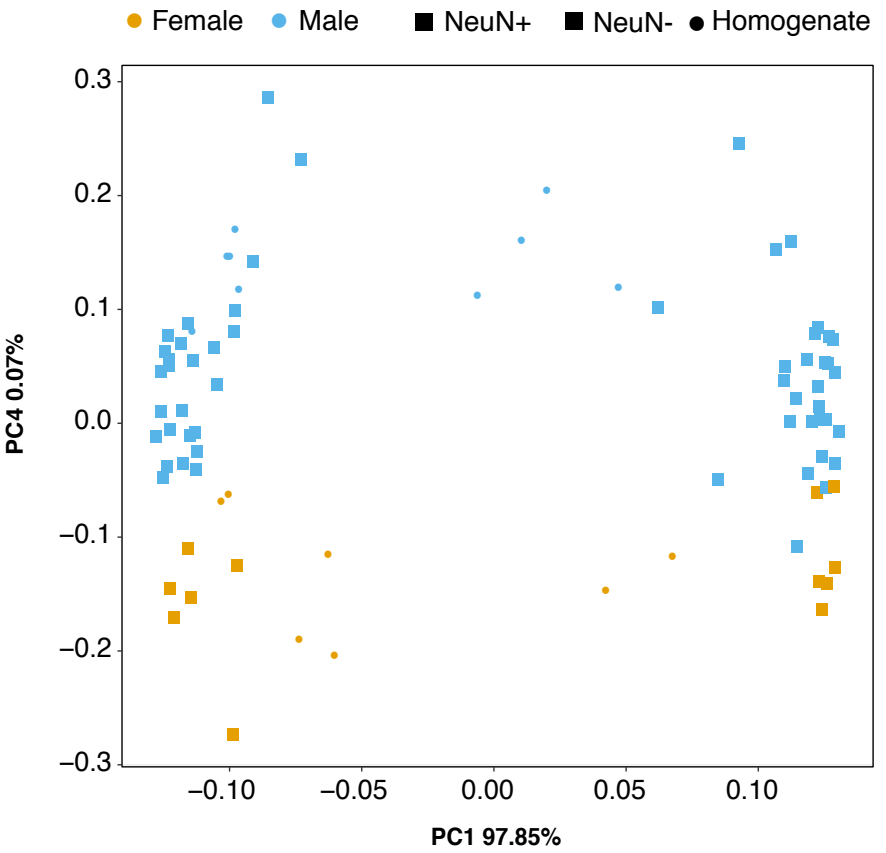

B

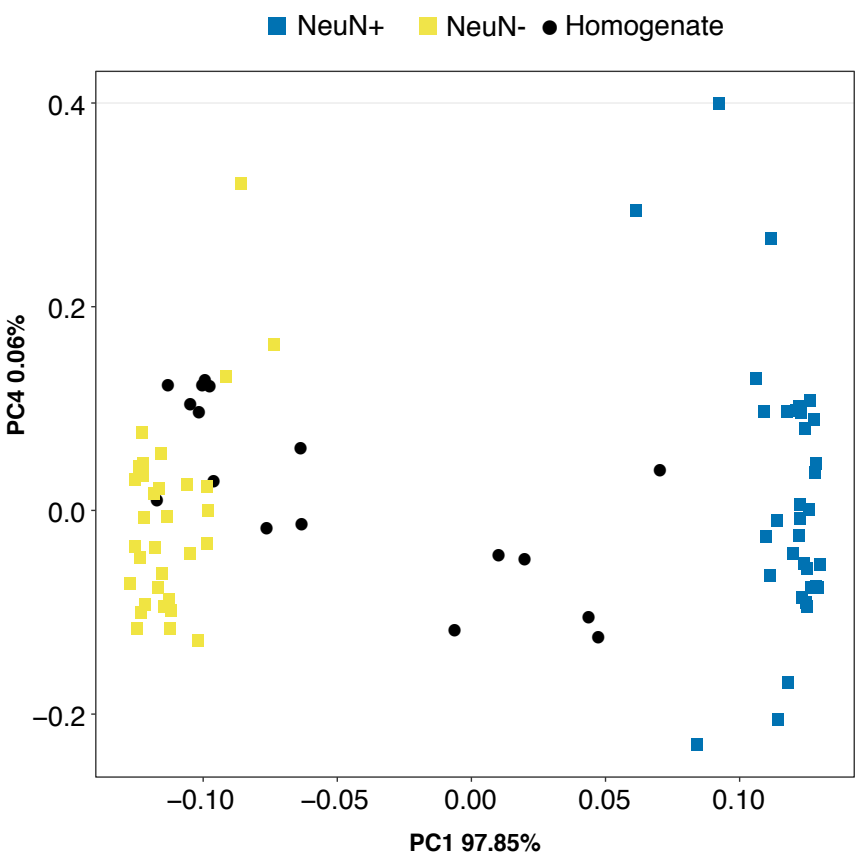

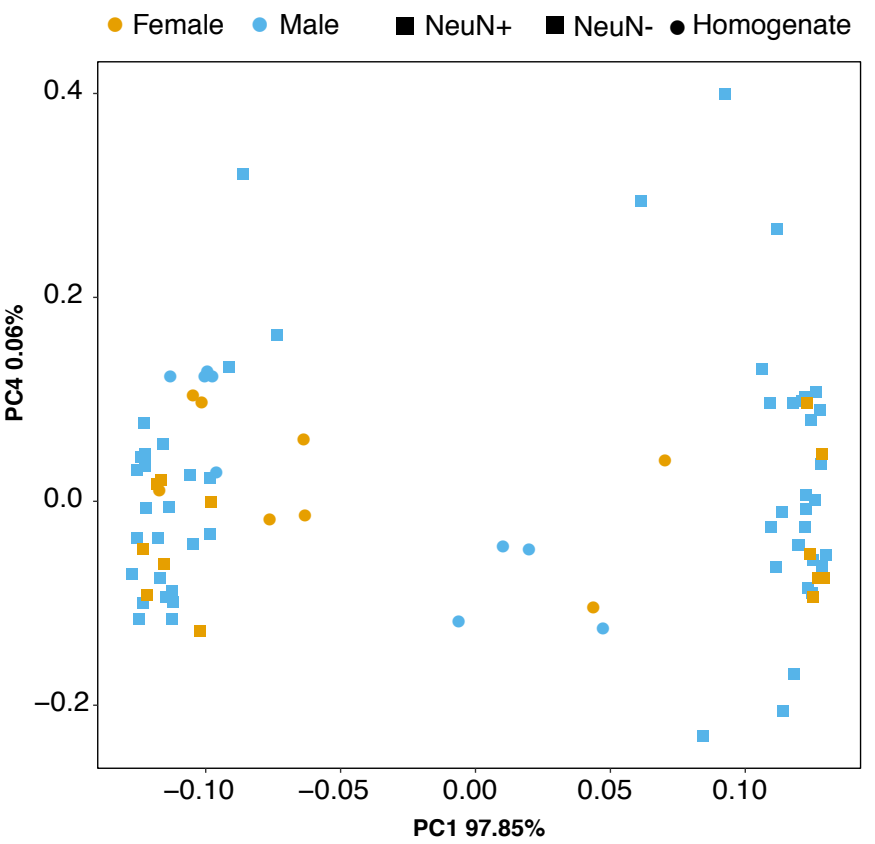

A **Figure S12** List of #peaks with signficant hQTLs (q value < 0.05)

	PFC NeuN+	PFC NeuN-	ACC NeuN+	ACC NeuN-	PFC HBCC Homog
H3K4me3	3412 (17)	3517 (17)	1565 (14)	3084 (15)	2077 (11)
H3K27ac	8042 (17)	6695 (17)	6731 (17)	7751 (15)	7207 (17)

*() No of samples

B List of #loci PGC GWAS SCZ overlap with hQTLs (qvalue <=0.05)

	PFC NeuN+	PFC NeuN-	ACC NeuN+	ACC NeuN-	PFC HBCC Homog
H3K4me3	8	8	3	8	2
H3K27ac	13	11	10	8	11

Figure S13

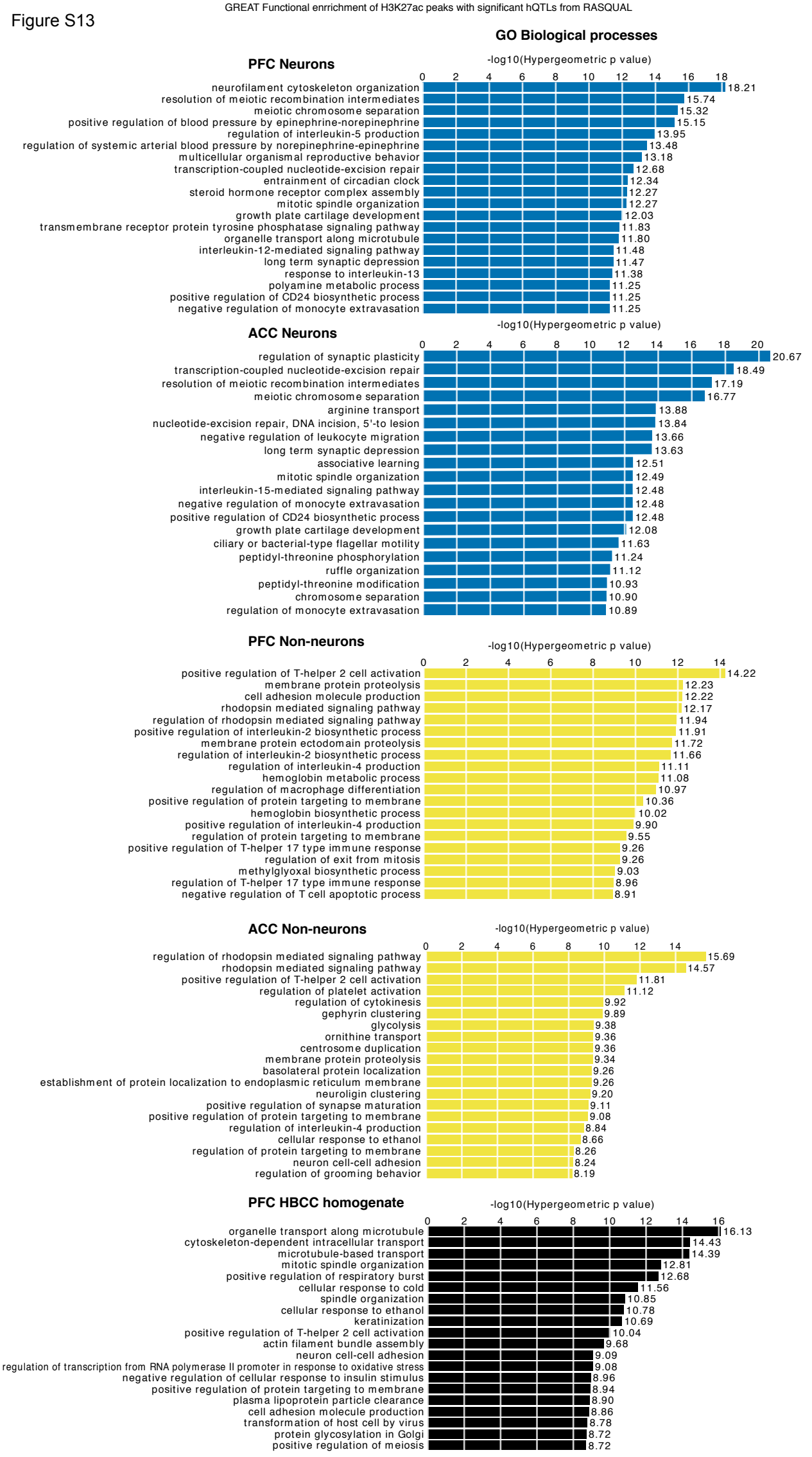
GREAT Functional enrrichment of H3K27ac peaks with significant hQTLs from RASQUAL
GO Biological processes
PFC Neurons
-log10(Hypergeometric p value)
0 2 4 6 8 10 12 14 16 18
neurofilament cytoskeleton organization 18.21
resolution of meiotic recombination intermediates 15.74
meiotic chromosome separation 15.32
positive regulation of blood pressure by epinephrine-norepinephrine 15.15
regulation of interleukin-5 production 13.95
regulation of systemic arterial blood pressure by norepinephrine-epinephrine 13.48
multicellular organismal reproductive behavior 13.18
transcription-coupled nucleotide-excision repair 12.68
entrainment of circadian clock 12.34
steroid hormone receptor complex assembly 12.27
mitotic spindle organization 12.27
growth plate cartilage development 12.03
transmembrane receptor protein tyrosine phosphatase signaling pathway 11.83
organelle transport along microtubule 11.80
interleukin-12-mediated signaling pathway 11.48
long term synaptic depression 11.47
response to interleukin-13 11.38
polyamine metabolic process 11.25
positive regulation of CD24 biosynthetic process 11.25
negative regulation of monocyte extravasation 11.25
ACC Neurons
-log10(Hypergeometric p value)
0 2 4 6 8 10 12 14 16 18 20
regulation of synaptic plasticity 20.67
transcription-coupled nucleotide-excision repair 18.49
resolution of meiotic recombination intermediates 17.19
meiotic chromosome separation 16.77
arginine transport 13.88
nucleotide-excision repair, DNA incision, 5'-to lesion 13.84
negative regulation of leukocyte migration 13.66
long term synaptic depression 13.63
associative learning 12.51
mitotic spindle organization 12.49
interleukin-15-mediated signaling pathway 12.48
negative regulation of monocyte extravasation 12.48
positive regulation of CD24 biosynthetic process 12.48
growth plate cartilage development 12.08
ciliary or bacterial-type flagellar motility 11.63
peptidyl-threonine phosphorylation 11.24
ruffle organization 11.12
peptidyl-threonine modification 10.93
chromosome separation 10.90
regulation of monocyte extravasation 10.89
PFC Non-neurons
-log10(Hypergeometric p value)
0 2 4 6 8 10 12 14
positive regulation of T-helper 2 cell activation 14.22
membrane protein proteolysis 12.23
cell adhesion molecule production 12.22
rhodopsin mediated signaling pathway 12.17
regulation of rhodopsin mediated signaling pathway 11.94
positive regulation of interleukin-2 biosynthetic process 11.91
membrane protein ectodomain proteolysis 11.72
regulation of interleukin-2 biosynthetic process 11.66
regulation of interleukin-4 production 11.11
hemoglobin metabolic process 11.08
regulation of macrophage differentiation 10.97
positive regulation of protein targeting to membrane 10.36
hemoglobin biosynthetic process 10.02
positive regulation of interleukin-4 production 9.90
regulation of protein targeting to membrane 9.55
positive regulation of T-helper 17 type immune response 9.26
regulation of exit from mitosis 9.26
methylglyoxal biosynthetic process 9.03
regulation of T-helper 17 type immune response 8.96
negative regulation of T cell apoptotic process 8.91
ACC Non-neurons
-log10(Hypergeometric p value)
0 2 4 6 8 10 12 14
regulation of rhodopsin mediated signaling pathway 15.69
rhodopsin mediated signaling pathway 14.57
positive regulation of T-helper 2 cell activation 11.81
regulation of platelet activation 11.12
regulation of cytokinesis 9.92
gephyrin clustering 9.89
glycolysis 9.38
ornithine transport 9.36
centrosome duplication 9.36
membrane protein proteolysis 9.34
basolateral protein localization 9.26
establishment of protein localization to endoplasmic reticulum membrane 9.26
neuroligin clustering 9.20
positive regulation of synapse maturation 9.11
positive regulation of protein targeting to membrane 9.08
regulation of interleukin-4 production 8.84
cellular response to ethanol 8.66
regulation of protein targeting to membrane 8.26
neuron cell-cell adhesion 8.24
regulation of grooming behavior 8.19
PFC HBCC homogenate
-log10(Hypergeometric p value)
0 2 4 6 8 10 12 14 16
organelle transport along microtubule 16.13
cytoskeleton-dependent intracellular transport 14.43
microtubule-based transport 14.39
mitotic spindle organization 12.81
positive regulation of respiratory burst 12.68
cellular response to cold 11.56
spindle organization 10.85
cellular response to ethanol 10.78
keratinization 10.69
positive regulation of T-helper 2 cell activation 10.04
actin filament bundle assembly 9.68
neuron cell-cell adhesion 9.09
regulation of transcription from RNA polymerase II promoter in response to oxidative stress 9.08
negative regulation of cellular response to insulin stimulus 8.96
positive regulation of protein targeting to membrane 8.94
plasma lipoprotein particle clearance 8.90
cell adhesion molecule production 8.86
transformation of host cell by virus 8.78
protein glycosylation in Golgi 8.72
positive regulation of meiosis 8.72

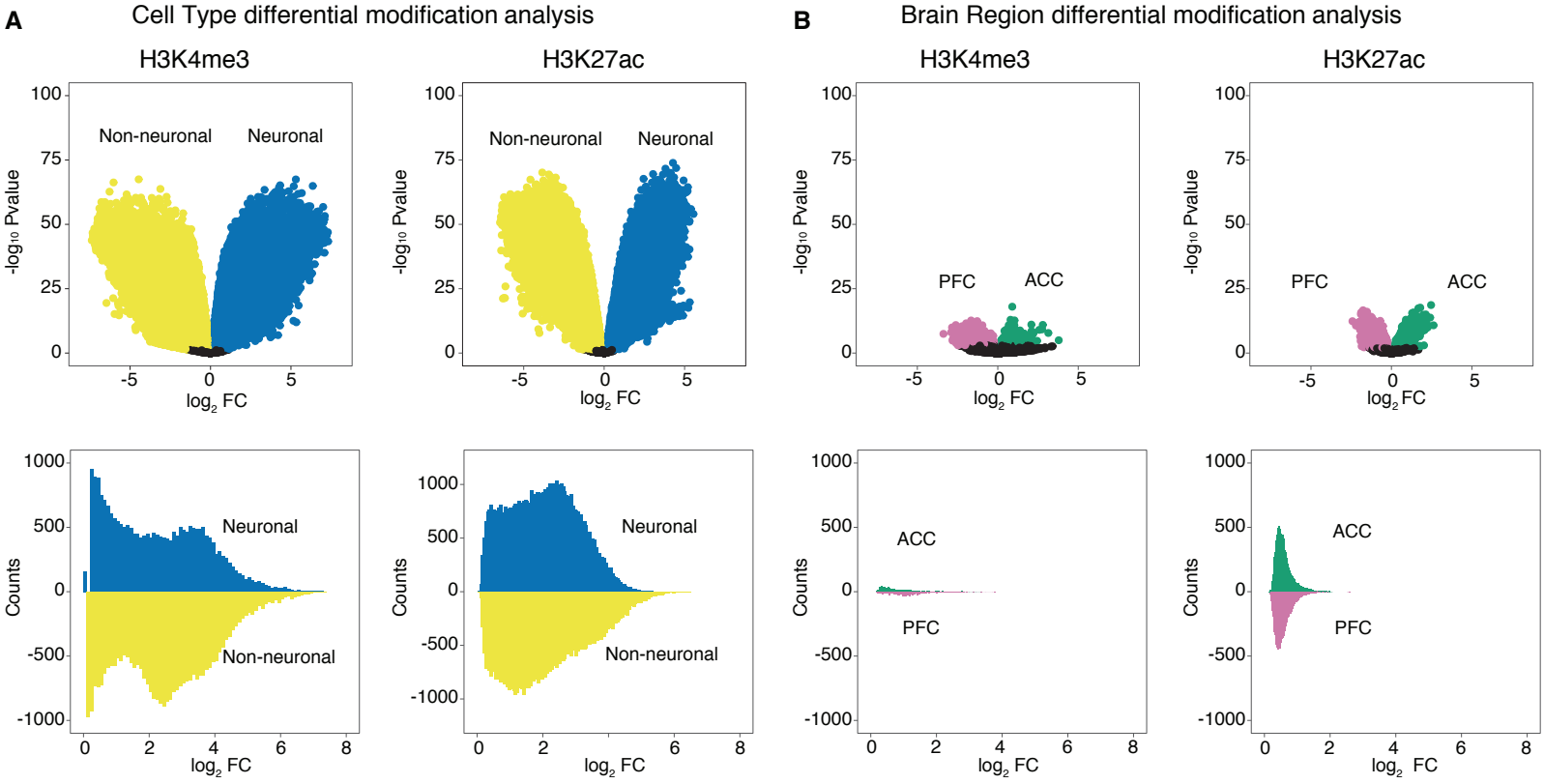
A
Cell Type differential modification analysis
H3K4me3
H3K27ac
Non-neuronal
Neuronal
-log10 Pvalue
log2 FC
Counts
B
Brain Region differential modification analysis
PFC
ACC

Figure S15

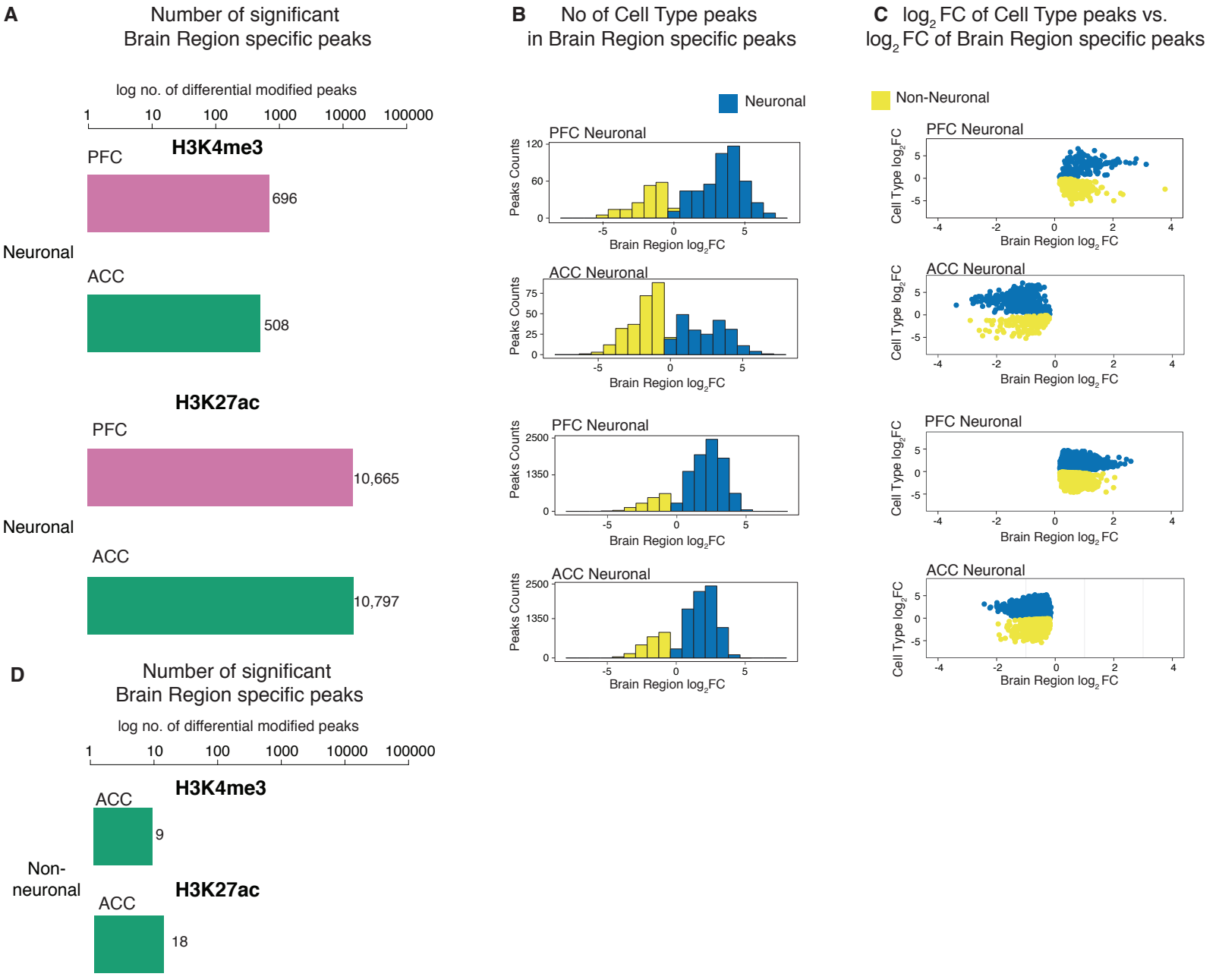
A
Number of significant
Brain Region specific peaks
log no. of differential modified peaks
1
10
100
1000
10000
100000
H3K4me3
PFC
696
Neuronal
ACC
508
H3K27ac
PFC
10,665
Neuronal
ACC
10,797
B
No of Cell Type peaks
in Brain Region specific peaks
Neuronal
PFC Neuronal
Peaks Counts
Brain Region log2FC
ACC Neuronal
C
log2 FC of Cell Type peaks vs.
log2 FC of Brain Region specific peaks
Non-Neuronal
Cell Type log2FC
D
Number of significant
Brain Region specific peaks
log no. of differential modified peaks
H3K4me3
ACC
9
Non-
neuronal
H3K27ac
ACC
18

Figure S16

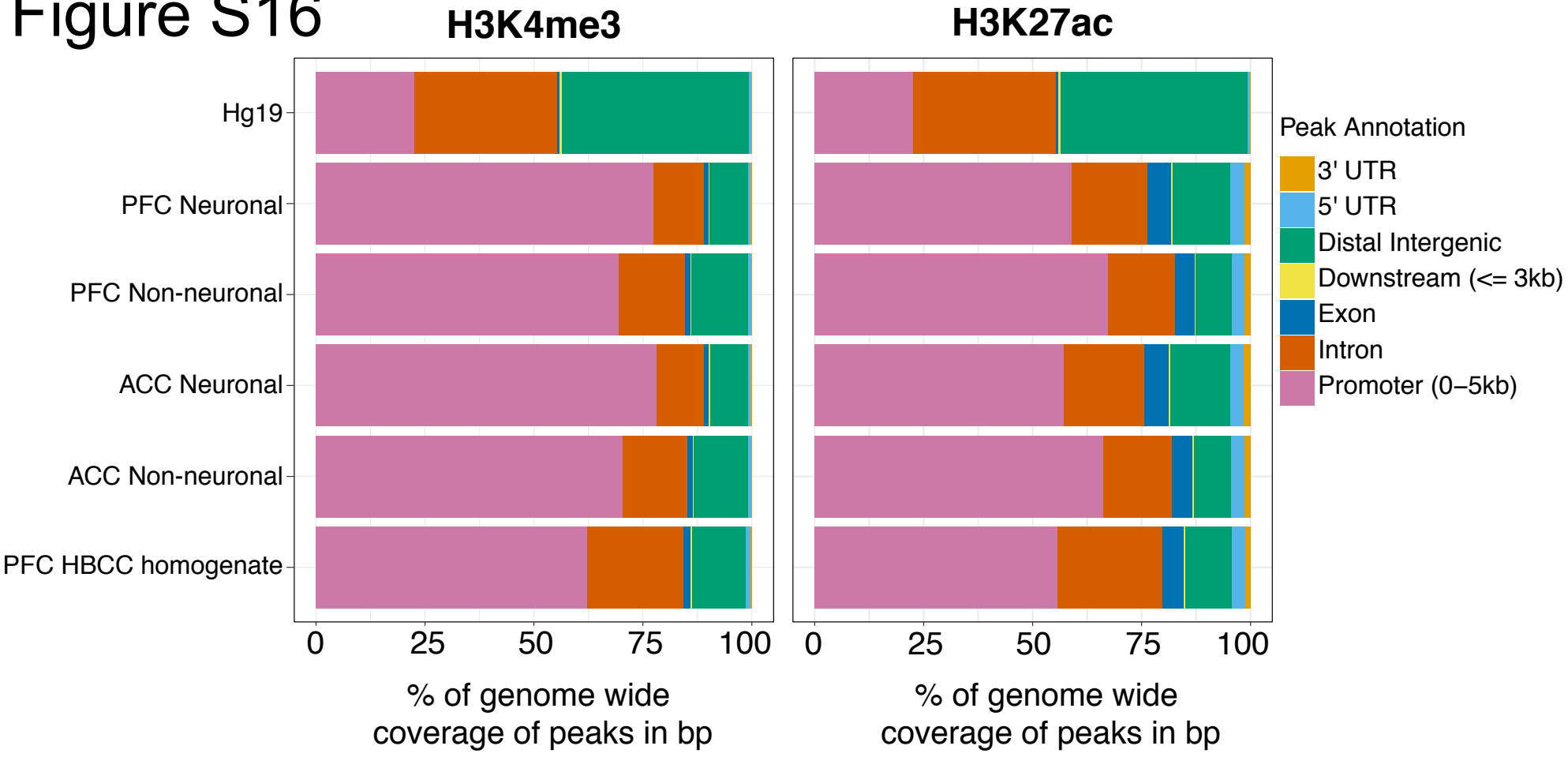
H3K4me3
H3K27ac
Hg19
PFC Neuronal
PFC Non-neuronal
ACC Neuronal
ACC Non-neuronal
PFC HBCC homogenate
0
25
50
75
100
% of genome wide coverage of peaks in bp
Peak Annotation
3' UTR
5' UTR
Distal Intergenic
Downstream (<= 3kb)
Exon
Intron
Promoter (0–5kb)

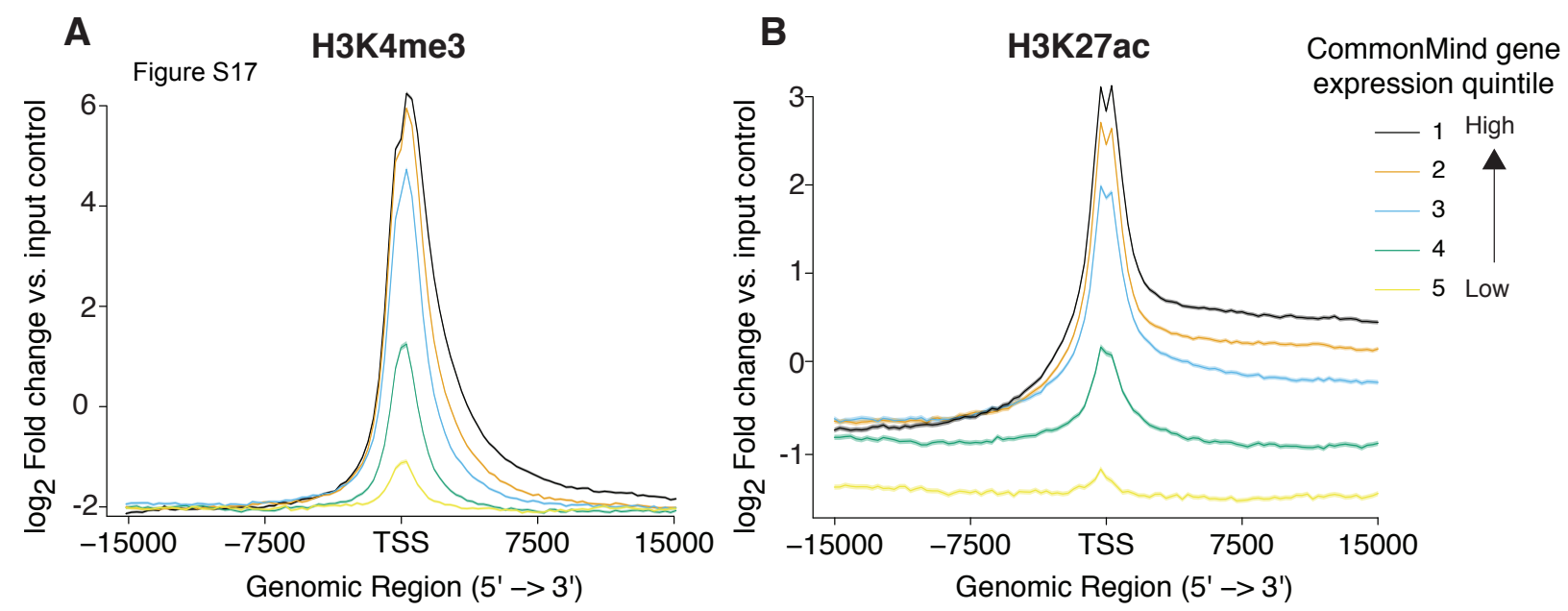
A
H3K4me3
Figure S17
log2 Fold change vs. input control
6
4
2
0
-2
−15000
−7500
TSS
7500
15000
Genomic Region (5' –> 3')
B
H3K27ac
log2 Fold change vs. input control
3
2
1
0
-1
−15000
−7500
TSS
7500
15000
Genomic Region (5' –> 3')
CommonMind gene expression quintile
1
2
3
4
5
High
Low

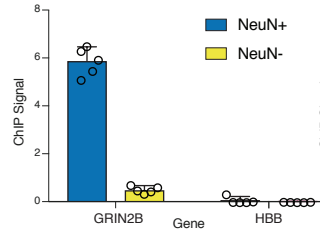
H3K4me3
NeuN+
NeuN-
ChIP Signal
8
6
4
2
0
GRIN2B
Gene
HBB

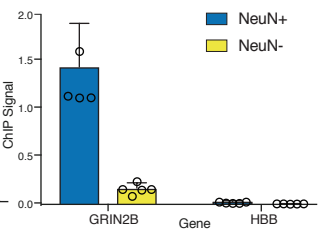
H3K27ac
NeuN+
NeuN-
ChIP Signal
2.0
1.5
1.0
0.5
0.0
GRIN2B
Gene
HBB

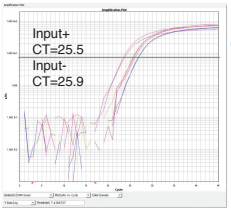
GRIN2B
Input+
CT=25.5
Input-
CT=25.9
NeuN+
CT=24.0
NeuN-
CT=27.6

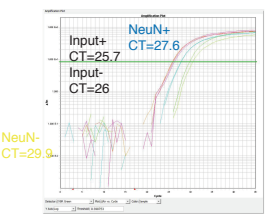
GRIN2B
Input+
CT=25.7
Input-
CT=26
NeuN+
CT=27.6
NeuN-
CT=29.9

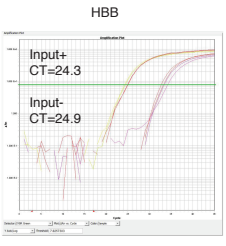
HBB
Input+
CT=24.3
Input-
CT=24.9
NeuN+
CT=32.9
NeuN-
CT=33.7

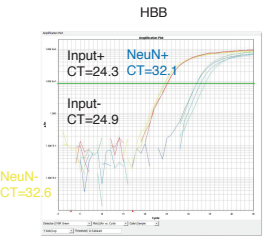
HBB
Input+
CT=24.3
Input-
CT=24.9
NeuN+
CT=32.1
NeuN-
CT=32.6

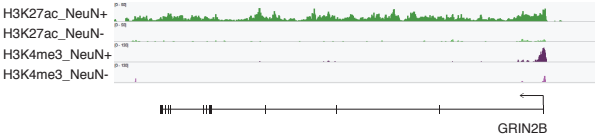
H3K27ac_NeuN+
H3K27ac_NeuN-
H3K4me3_NeuN+
H3K4me3_NeuN-
GRIN2B

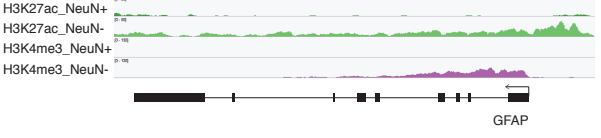
H3K27ac_NeuN+
H3K27ac_NeuN-
H3K4me3_NeuN+
H3K4me3_NeuN-
GFAP


H3K27ac_NeuN+
H3K27ac_NeuN-
H3K4me3_NeuN+
H3K4me3_NeuN-
HBB

Figure S19

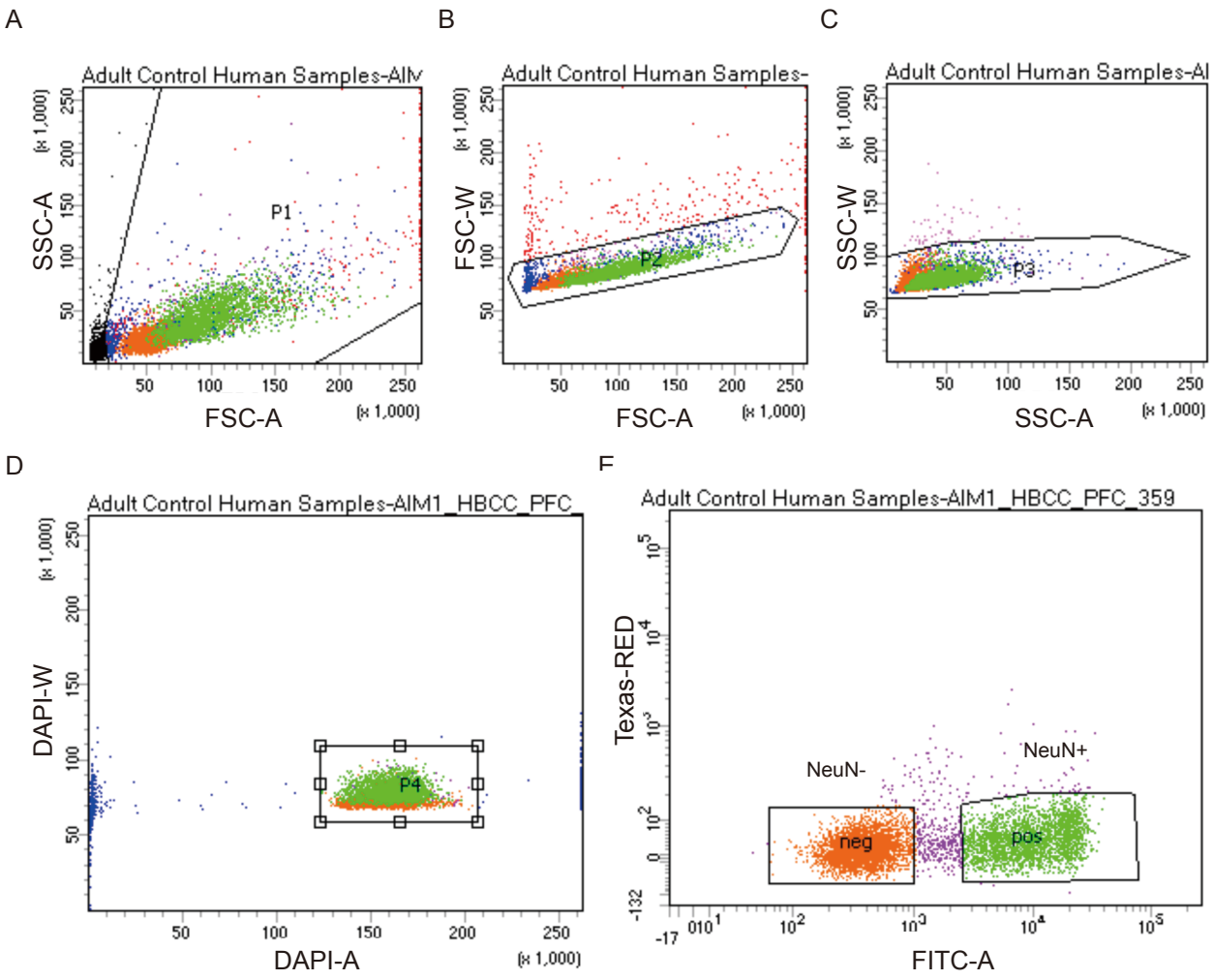
A
Adult Control Human Samples-AIM
SSC-A
(x 1,000)
P1
FSC-A
(x 1,000)
B
Adult Control Human Samples-
FSC-W
P2
FSC-A
(x 1,000)
C
Adult Control Human Samples-AI
SSC-W
P3
SSC-A
(x 1,000)
D
Adult Control Human Samples-AIM1_HBCC_PFC
DAPI-W
P4
DAPI-A
(x 1,000)
F
Adult Control Human Samples-AIM1_HBCC_PFC_359
Texas-RED
NeuN-
NeuN+
neg
pos
FITC-A